Vietnamese-German University

COPYRIGHT WARNING

This paper is protected by copyright. You are advised to print or download **ONE COPY** of this paper for your own private reference, study and research purposes. You are prohibited having acts infringing upon copyright as stipulated in Laws and Regulations of Intellectual Property, including, but not limited to, appropriating, impersonating, publishing, distributing, modifying, altering, mutilating, distorting, reproducing, duplicating, displaying, communicating, disseminating, making derivative work, commercializing and converting to other forms the paper and/or any part of the paper. The acts could be done in actual life and/or via communication networks and by digital means without permission of copyright holders.

The users shall acknowledge and strictly respect to the copyright. The recitation must be reasonable and properly. If the users do not agree to all of these terms, do not use this paper. The users shall be responsible for legal issues if they make any copyright infringements. Failure to comply with this warning may expose you to:

- Disciplinary action by the Vietnamese-German University.
- Legal action for copyright infringement.
- Heavy legal penalties and consequences shall be applied by the competent authorities.

The Vietnamese-German University and the authors reserve all their intellectual property rights.

RUHR-UNIVERSITÄT BOCHUM

MechEng
Mechanical Engineering

Vietnamese-German University

DEVELOPENT OF A MR BRAKE WITH JIG-JAG MAGNETIC FLUX-LINE

BACHELOR THESIS

BINH DUONG 4.1.2019

Vietnamese-German University

Submitted by: Bui Van Dang

RUB Student ID: 108018206866

VGU Student ID: 9707

Supervisor: Prof. Dr. Nguyen Quoc Hung

ABSTRACT

This thesis presents an optimized design for a magneto rheological fluid brake (MRB) for industrial applications. The actuator consists of a disk that is immersed within the magneto rheological fluid (MRF) surrounded by an electromagnet. The braking torque is controlled by changing the DC current applied to the electromagnet. In the presence of a magnetic field, the magneto rheological fluid particle aligns in a chain like structure, so increasing the viscosity. The shear stress generated by the rheological fluid causes friction within the surfaces of the rotating disk. Electromagnetic analysis of the proposed system is carried out using finite element based ANSYS software and the amount of magnetic field generated is calculated with the help of ANSYS. The geometry of the brake is optimized and performance of the system in terms of braking torque is carried out. Proposed design reveals higher performance in terms of braking torque from the existing literature.

Table of contents

Abbreviations

MR	Magnetorheological
MRF	Magnetorheological fluid
MRB	Magnetorheological brake
FEM	Finite element method

List of figures

List of tables

Symbols

τ	Shear stress
τ_y	Yield stress
η	Newtonian viscosity
$\dot{\gamma}$	Shear rate
K	Consistency index
m	Flow index
Y	A rheological parameter of MRF
α	Saturation moment index
n	Velocity profiles of the post-yield flow regions
Ω	Angular velocity of the disc
R	Radius from ends of the slotted groove to the brake shaft
L_a	Length of a slotted projection on an axis
Φ	Angle between the groove and the axis
L	Length of the groove
L_C	Frictional length of the seals surface
R_S	Outer diameter of the seal.
f_C	Friction per unit length of seal circumference
f_h	Frictional force of the seal
A_r	Inner diameter of the seal.
H_k	Strength of the magnetic field at the k^{th} link of the circuit
l_k	Useful length of that link
N_{turns}	Number of turns of the coils

I	Amperage
Φ	The magnetic flux of the circuit
B_k	Magnetic flux density at the kth link
A_k	Cross sectional area at the kth link
μ_0	The permeability of free space ($\mu_0 = 4\pi 10^{-7}$ *Tm/A*)
μ_k	Relative permeability of the material at the kth bond
μ_{mr}	Relative permeability of MRF
μ	Relative permeability of materials
m_b	Mass of MRB
V_b	Volume of MRB
ρ_b	Density of MRB
$B(s)$	Magnetic flux density at each node on the curve
S	Dummy variable for the integral.
OBj_o	Reference target values
Q	Feedback surface parameter to accommodate constraints
P_x	Outer penalty function, applies to variable x
P_g	Extended internal penalty function, applied to the g state variable

1. Introduction

This chapter gives us an overview of the MRF brake and its application in reality. Besides its strengths, challenges and difficulties in creating a new type of brake are mentioned adequately. After acknowledging what attributes and difficulties, a straight plan is sketched out in detail to keep the progress toward the appropriate goal correctly.

1.1 Overview and Motivation

Nowadays, there are two main types of brakes: oil brake and mechanical brake. Each type of brake has different design and usage characteristics. Brake pads of mechanical brakes are traditional types, using the mechanism of direct transmission from the hand brake or foot brake to the pads, pressing the brake pads and brake discs to increase friction, reduce the speed of the vehicle. Meanwhile, the oil brake is a hydraulic piston system, when the user squeezes the brake, the hydraulic system of the brake will squeeze the two brake pads into the brake disc to reduce the speed. Both types of brakes use friction mechanisms between the brake pads and the brake discs to slow down and so it has the following defects: brake pads wear quickly, making noise, etc. Currently, even advanced brakes do not completely fix these problems.

On the other hand, the introduction and research and development of MRF applications have created opportunities to develop a new type of brake not only for cars and motorcycles but also for many other applications, to be able to overcome the disadvantages of traditional brakes. MRF brake has been researched and applied widely all over the world, including some of the typical brakes such as disc brakes, drum brakes, T-disc brakes, brakes with side coils, …. Therefore, with the outstanding features and advantages of MRB compared to the current brakes and the research and application of MRB are positive, highly feasible, in accordance with the actual conditions and needs today, so I have the research topic "Development of MR brake with jig-jag magnetic flux line".

1.2 Goal and Scope

As we know, braking is an important mechanism in almost all machines, helping to control the speed and be widely applied around the world. But for the current brakes, the disadvantages are: loud noise, generates a lot of heat during operation, wears quickly, gets stuck, ... Therefore, to overcome the above disadvantages, MRF brakes are researched with the following outstanding improvements: fast response time, low operating energy, simple design and structure, no wear and tear due to very small friction, easy to control, …The goal of the project is to design and manufacture fluid braking systems from the new generation to replace existing brakes with many outstanding features and advantages.

In this study, I conduct a theoretical approach combined with practical requirements to propose a new generation MRF brake configuration. Since then, I conduct verification by simulation based on theoretical calculations to come to empirical verification to compare and evaluate the features and effectiveness of the proposed MRF brakes. Methodological analysis from related scientific works recently published in scientific journals, national and international scientific conferences, on dissertations and related documents. The methodology is implemented according to the following diagram:

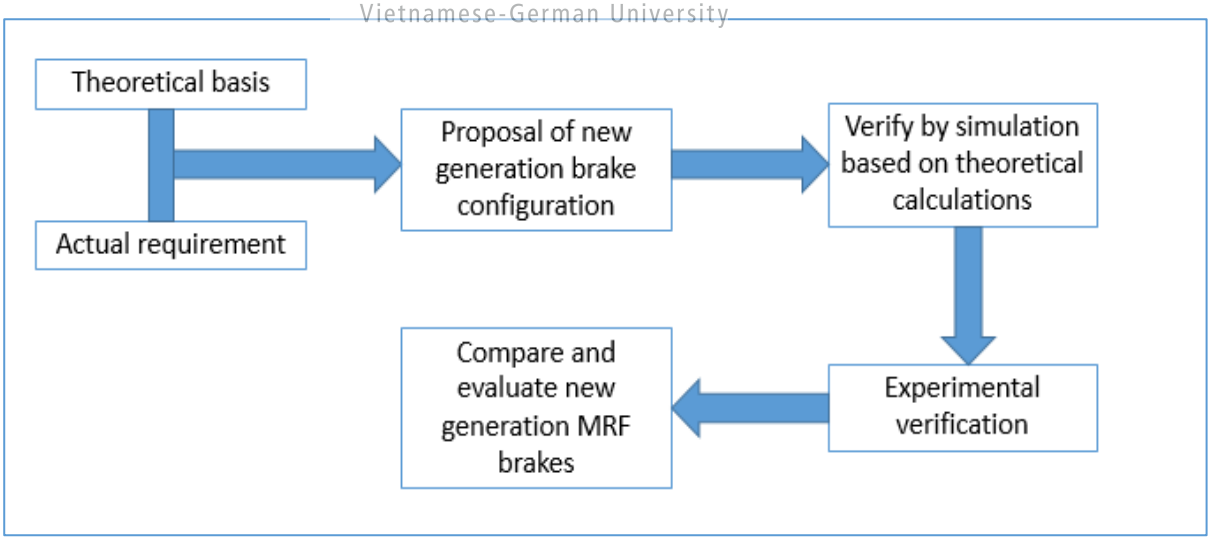

Figure 1- 1: Methodological diagram

2. Fundamental and state of research

In this chapter, the aim of citing the studies and works from documents and papers associated with the MRB design topic to analyze and learn special features of magnetorheological fluid (MR fluid, or MRF). Based on that, the idea of developing a new generation optimizes the MRF brake pros and reduces its cons.

2.1 Introduction to magnetorheological fluid and applications

Magnetorheological fluid is a type of smart fluid discovered in 1940 by J. Rabinow. However, until 1990, after improvement and development, MR fluid could be applied widely. Magnetorheological fluid consists of three main components:

- Soft iron particles (occupy a small portion of mass from 20% to 45%), The magnetic particles are iron carbonyl particles because of their high saturation. The carbonyl iron particles are obtained by decomposing iron pentacarbonyl $Fe(CO)_5$ resulting in spherical shaped particles with a diameter of 1-10 µm. The spherical particles make it less abrasive, harder, and more durable. In particular, these particles are covered with an outer layer of 97.8% metal, and the process to obtain these carbonyl particles is expensive, so other low-cost treatment technologies are being studied such as atomization.
- Carrier liquid is selected based on its viscosity, operating temperature, compatibility with other liquid components. Usually, the base fluid is hydrocarbon oil, mineral oil, synthetic oil, …due to the durable, popularity in the market and the availability of additives
- Additives have many formulas; different mixing ratios are usually exclusive for each type of fluid. In general, the additives have the function of solving problems such as deposition, agglomeration, preventing oxidation, reducing the abrasion of ferromagnetic particles.

Aggregation of these parts forms a homogeneous mixture that determines maximum yield stress, permeability, and operating temperature range. Therefore, there are many different types of MRF on the market today.

2.2 Principle of MRF

In a normal state, when no magnetic field is passed through the fluid, the ferromagnetic particles in the fluid move freely and exhibit Newton properties like other liquids. In a state in which the external magnetic field is applied, the ferromagnetic particles in the fluid will coalesce and rearrange together in the shape of magnetic field lines capable of resisting the breaking of bonds. The strength of the bonds depends on the magnitude of the applied external magnetic field

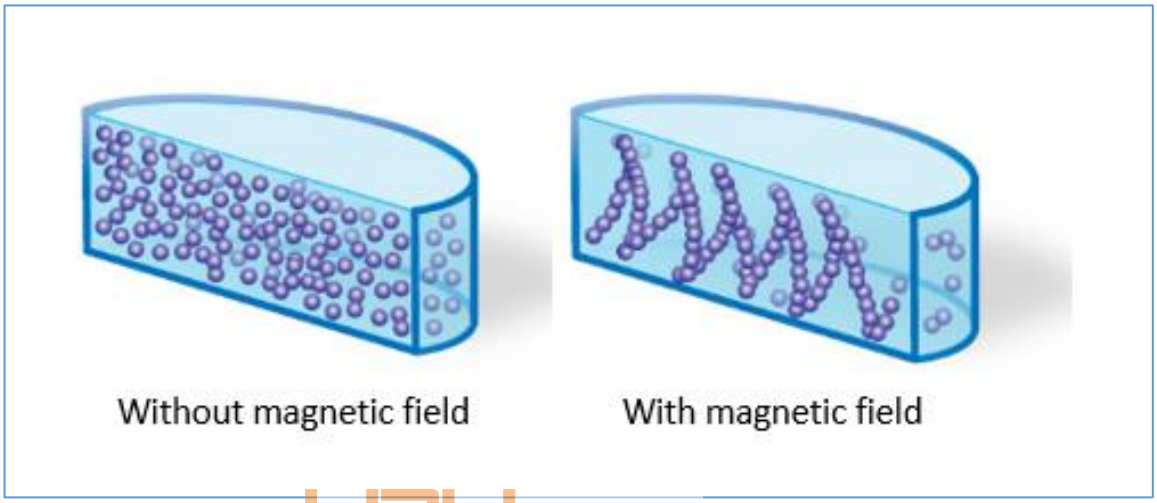

Figure 2- 1: The bond between particles varies with the magnetic field

The yield shear stress is the main figure of the advantage of MR fluid and derives from the non-Newtonian behavior of those fluids. The MR fluid behaves following an alleged Bingham law or Herchel-Bulkley law.

The Bingham law suggests that it exhibits a non-zero shear stress value for a zero shear rate, behaving additional sort of a solid than sort of a liquid, as shown in Figure 2-2. The value of the shear stress at no shear rate is termed yield stress of the MR fluid and is controlled by the applied magnetic field; the larger the field, the higher the yield stress. The higher the yield stress the upper the force the material will stand up to while not flowing. Bearing a load is feasible solely as a result of MR fluids will modify their aggregations states ever-changing from a viscous free-flow liquid to a similar solid state. The formula for shear stress is expressed as follows:

$$\tau = \tau_y(H)sgn(\dot{\gamma}) + \eta(\dot{\gamma}) \qquad (2\text{-}1)$$

Where: τ: Shear stress

τ_y: Yield stress

η: Newtonian viscosity

$\dot{\gamma}$: Shear rate

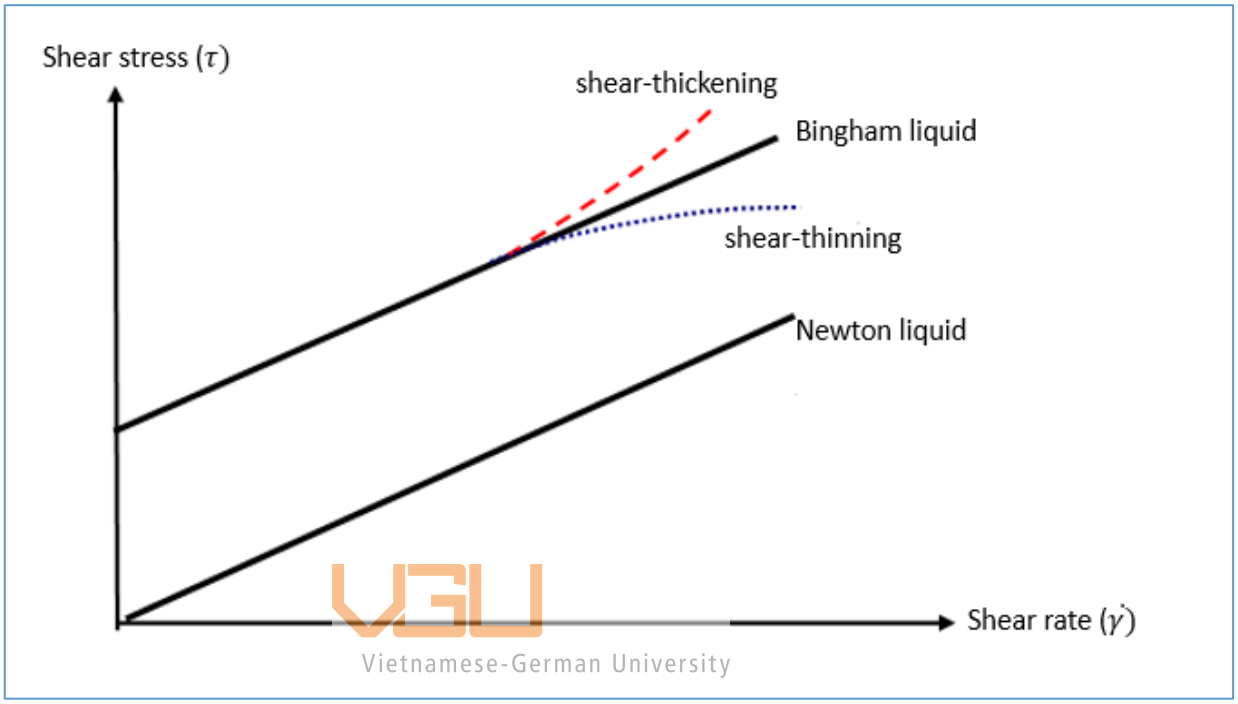

Figure 2- 2: Correlation between Newton liquid and Bingham liquid

Herchel-Bulkley law was introduced by Winslow Herschel and Ronald Bulkley in 1926. In this case, the liquid will either shear-thinning or shear-thickening, especially when the MRF is subject to a high shear rate. Herchel-Bulkley law is shown as follows:

$$\tau = (\tau_y(H)sgn(\dot{\gamma}) + K|\dot{\gamma}|^{\frac{1}{m}})sgn(\dot{\gamma}) \quad (2\text{-}2)$$

Where K: Consistency index

m: Flow index

For m < 1 the fluid is shear-thinning, whereas for m > 1 the fluid is shear-thickening. If m = 1 this model reduces to the Newtonian fluid. In many studies, it is shown that the parameters K, μ, τ are constant. But in reality, these parameters are affected by magnetic fields. The

rheological properties of MRF depend on the magnetic field and can be estimated by the following formula:

$$Y = Y_\infty + (Y_0 - Y_\infty)(2e^{-B\alpha_{SY}} - e^{-2B\alpha_{SY}}) \quad (2\text{-}3)$$

In which Y stands for a rheological parameter of MRF such as yield stress, viscosity, consistency parameter, liquid coefficient. The value of the Y parameter tends to be from zero to the saturation value which is the saturation torque factor of Y. Basic parameters of the Bingham, Herschel-Bulkey model of MRF are based on the experiments shown in Table 2-1

Table 2- 1: Basic parameters of MRF

	MRF-122-2ED	MRF-132DG	MRF-140CG
Bingham model	$\mu_0 = 0.075 pa.s$; $\mu_\infty = 2.8 pa.s$ $\alpha_{s\mu} = 4.5T^{-1}$ $\tau_{y0} = 12 pa$; $\tau_{y\infty} = 25200 pa$; $\alpha_{st_y} = 2.9T^{-1}$	$\mu_0 = 0.1 pa.s$; $\mu_\infty = 3.8 pa.s$; $\alpha_{s\mu} = 4.5T^{-1}$ $\tau_{y0} = 15 pa$; $\tau_{y\infty} = 40000 pa$; $\alpha_{st_y} = 2.9T^{-1}$	$\mu_0 = 0.29 pa.s$; $\mu_\infty = 4.4 pa.s$; $\alpha_{s\mu} = 5T^{-1}$ $\tau_{y0} = 25 pa$; $\tau_{y\infty} = 52000 pa$; $\alpha_{st_y} = 3T^{-1}$
Herschel-Bulkey Model	$K_0 = 0.15 pa.s^n$; $K_\infty = 3200 pa.s^n$; $\alpha_{sk} = 5T^{-1}$ $\tau_{y0} = 6 pa$; $\tau_{y\infty} = 16000 pa$; $\alpha_{st_y} = 2T^{-1}$ $n_0 = 0.917$; $n_\infty = 0.25$; $\alpha_{sn} = 30$	$K_0 = 0.22 pa.s^n$; $K_\infty = 3900 pa.s^n$; $\alpha_{sk} = 5T^{-1}$ $\tau_{y0} = 10 pa$; $\tau_{y\infty} = 30000 pa$; $\alpha_{st_y} = 2T^{-1}$ $n_0 = 0.917$; $n_\infty = 0.25$; $\alpha_{sn} = 32$	$K_0 = 0.65 pa.s^n$; $K_\infty = 5400 pa.s^n$; $\alpha_{sk} = 5T^{-1}$ $\tau_{y0} = 25 pa$; $\tau_{y\infty} = 39000 pa$; $\alpha_{st_y} = 2T^{-1}$ $n_0 = 0.915$; $n_\infty = 0.24$; $\alpha_{sn} = 35$

2.3 Typical using modes for MR fluids

In order to take advantage of MR fluids properties, there are 3 main ways are used in current engineering applications: flow mode, shear mode, and squeeze mode

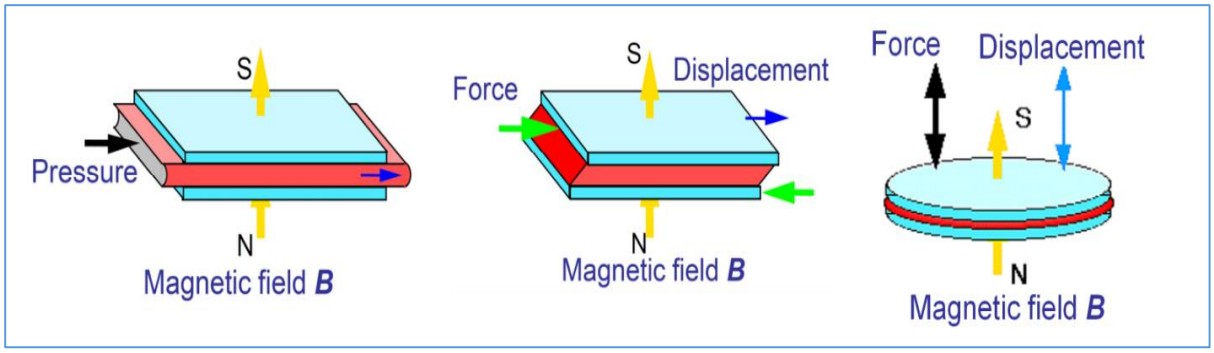

Figure 2- 3: Model of MRF

Flow mode, conjointly known as valve mode, exploits the fluid between two fastened walls. The flow mode's magnetic field is normal to the flow directions and is typical for linear damper applications.

Shear mode is principally utilized in rotary applications like brakes and clutches and therefore the fluid is strained between two walls that are in relative motion with the magnetic field normal to the wall direction.

Squeeze mode mostly used in bearing applications, it can deliver low displacements and high force. The magnetic field of squeeze mode normal to wall directions.

All three modes have the same working principle: The fluid's apparent viscosity is changed by the applied magnetic field regulates the yield stress. So the quantity of dissipated energy of the system is just manageable by engaged on the coil current and also the system will give semi-active behavior.

2.4 Applications of magnetorheological fluids

The magnetorheological fluids are attractive for braking, damping and dissipative devices due to the sudden change in the MR behavior just about millisecond as a result of the magnetic field application. The MR fluids can make to build silent, integral, quick mechanical systems strengthen by means of electronic controls. There are three main ways to take advantage of the MR fluids in engineering applications.

Damper using MRF

Damper is an indispensable part of the car as well as many other machines, it has the effect of protecting elastic parts along with quenching vibrations. Most conventional dampers have a constant hardness, so if the surface roughness of the pavement coincides with the vibration frequency of the damping device or the surface undulation is too large, the effect will be greatly reduced or even disabled.

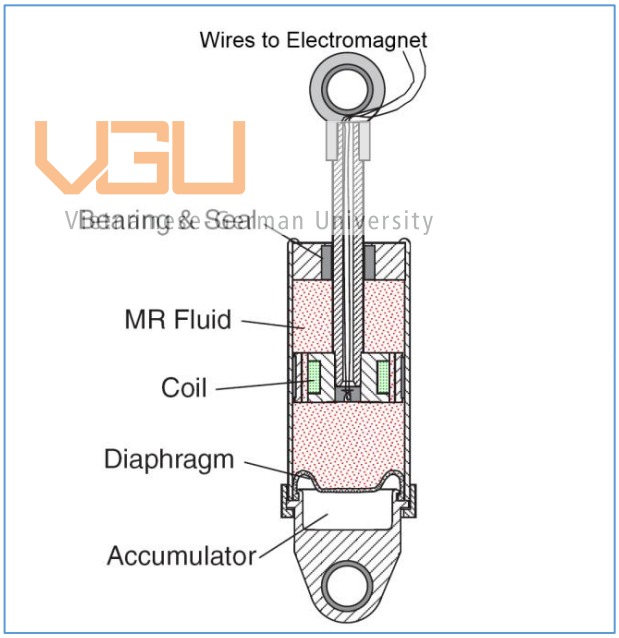

Figure 2- 4: Damper using MRF

The main asset of an MR based damper is the controllability of the system, which can be adjusted in order to provide the desired level of damping by simply changing the current. The main plan is to get the specified level of damping by variable the magnetic induction in a passage between two separated MR fluid chambers. The applications of the one over damper are primarily within the vibration suppression of mechanical elements like seat suspension, automobile suspensions, and industrial vibration suppression, whereas the double over damper is principally used for bicycle applications, gun recoil applications, and for stabilizing buildings

and bridges throughout earthquakes. The output forces of such a device will vary from quite low forces (hundreds of Newton) of light suspension up to twenty tons in the class of civil applications, during which they have to recoup the improbably massive forces caused by the shaking of entire buildings.

Magnetorheological brake

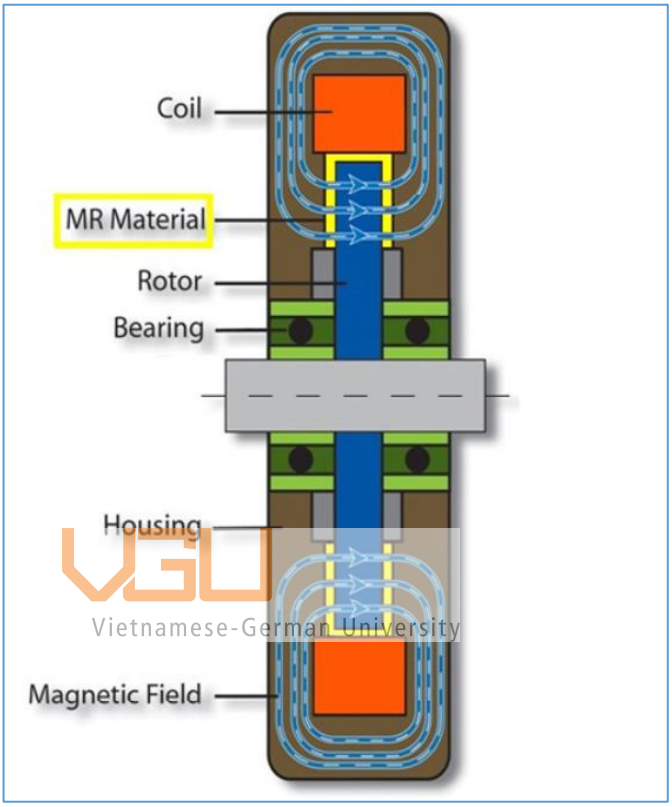

Figure 2- 5: Traditional MRB

Magnetorheological fluid is located between the brake disc and the brake cover. When supplying electricity to the coil, the coil will generate a magnetic field through the fluid which makes plasticizer and increase the frictional stress between the surface of the brake disc and the brake cover, creating the brake moment. Not any moving part is used to change the transmitted torque and the torque value can be smoothly controlled through the coil current. Even though multi-disc applications are often used to increase the output force, the standard application MR brake devices are within the high faultlessness and low power range.

Engine mount using MRF

Engine mount mechanism is an important part of cars, ships ... it is used to mount the engine on the chassis and ensure the engine and transmission parts operate durably. The engine mount is also used to reduce the vibration from the engine to the chassis so that the occupants feel more comfortable. Many types of engine mounts have been researched and developed, some of which have been put into production and marketed. The classification of engine mounts can be based on the impact of external energy sources, the engine mounts can be divided into three categories: passive mount, active mount, semi-active mount.

There have been many recent studies on semi-active motor mounts using MRF. Thanks to its controllability, MRF can fully meet the requirements of adjusting the damping force in the mounting mechanism. Figure 2-6 is a model of mechanical jigs. It works like a damping, when the electricity goes through the coil, the fluid in the channel becomes plasticized. The change of current shifts the hardness of fluid in the channel.

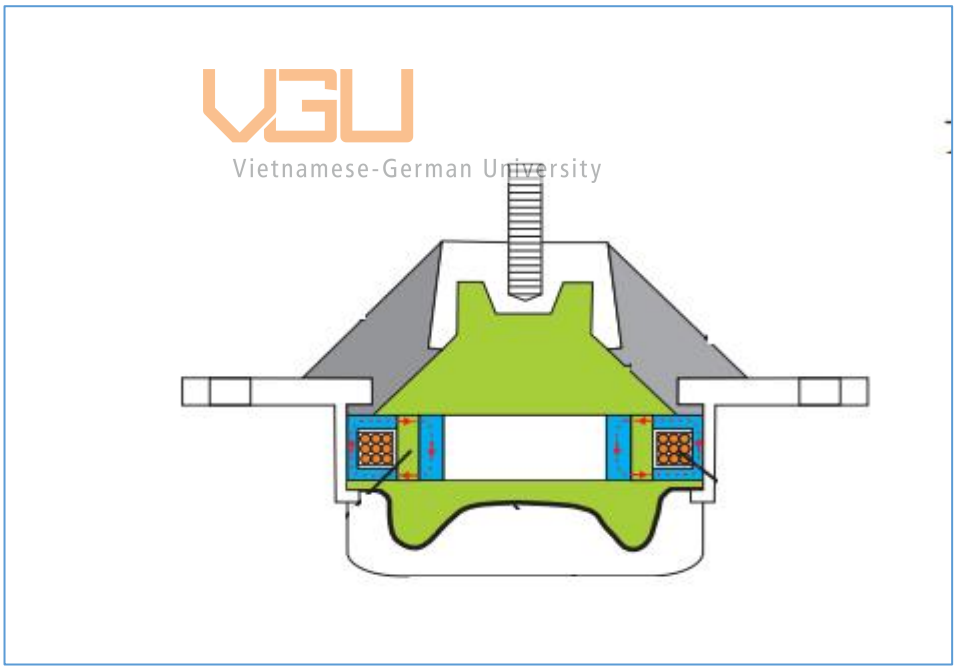

Figure 2- 6: Engine mount using MRF

Haptics using MRF

Haptics is a term with the same meaning as the haptic feedback system. It makes it possible to feel like you are directly holding or doing something even though we are far away and only observing directly through the camera. Thanks to its quick response, MRF has been quickly researched and applied in this area, particularly MR gloves. The essence of MR gloves is a combination of many MRB, which block the movement of the fingers in proportion to the actual feedback force. From there the gloved person can feel like being directly manipulated. Today Haptics is being used quite widely, especially in the field of medicine, which helps a doctor to perform important operations remotely.

Figure 2- 7: Haptics using MRF

Valve using MRF

Another application of MRF is the MR valve. MR valves are similar to other valves, but they are simpler and easier to handle. Initially, without the effect of the magnetic field, the fluid flowed into the valve according to the inlet, passing through the slits and outward as the outlet. When there is a magnetic field in effect, the fluid flow around the coil is magnetized and becomes linked together. Only when the pressure of the fluid flow is large enough to overcome

this bonding force, the fluid flow through the valve. When the magnetic field is large enough, the fluid around the coil solidifies so that it cannot flow through the valve.

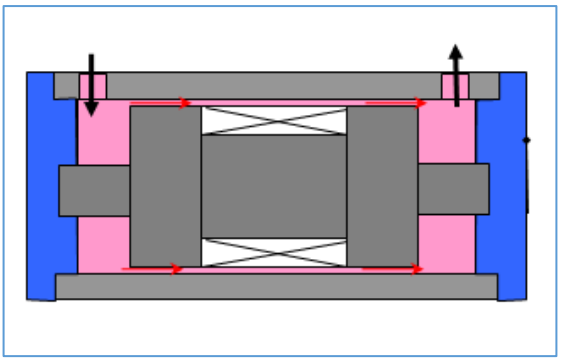

Figure 2- 8: Valve using MRF

2.5 Type of brake using MRF

There have been several studies related to MRB shapes aimed at optimizing braking performance, including the following.

Disc brake: is the most common type of brake and also the first design of MRB. This is a standard brake to be marketed. The advantage is easy to fabricate and achieve optimal results in terms of weight and dimensions. However, this application is not suitable in the case of the installation location of cylindrical MRB is long and small

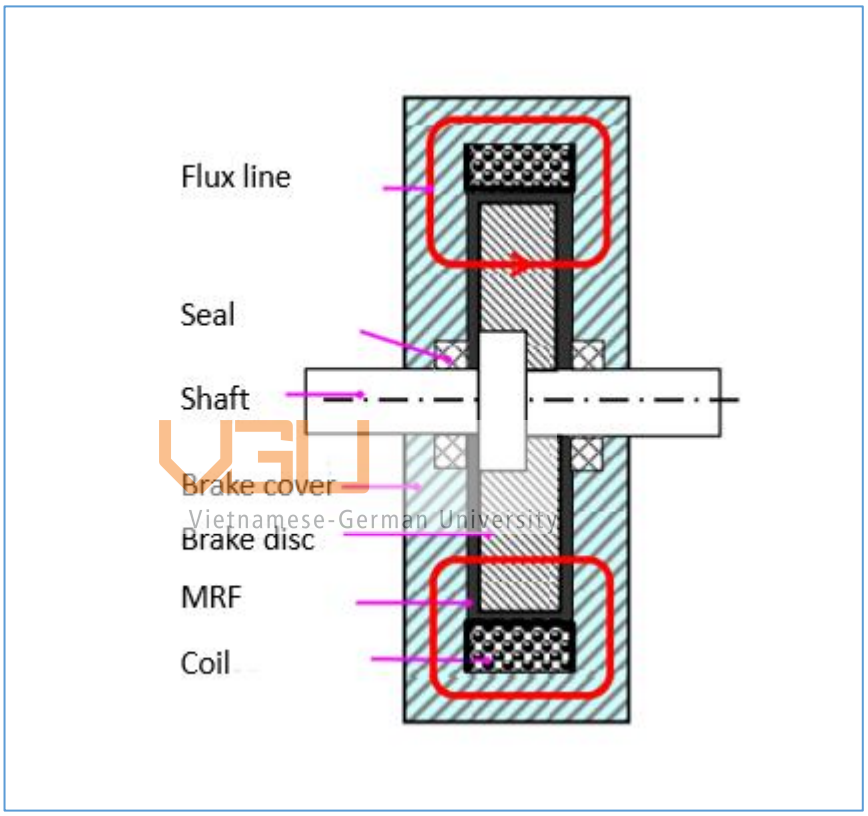

Figure 2- 9: Disc brake

Drum brake: Drum brake is possible to overcome the disadvantages of the above type of brake because the braking force is generated on the cylinder surface of the drum, however, it creates a quite large moment of inertia. To overcome this problem, the inverted drum shape was designed and greatly reduced the moment of inertia.

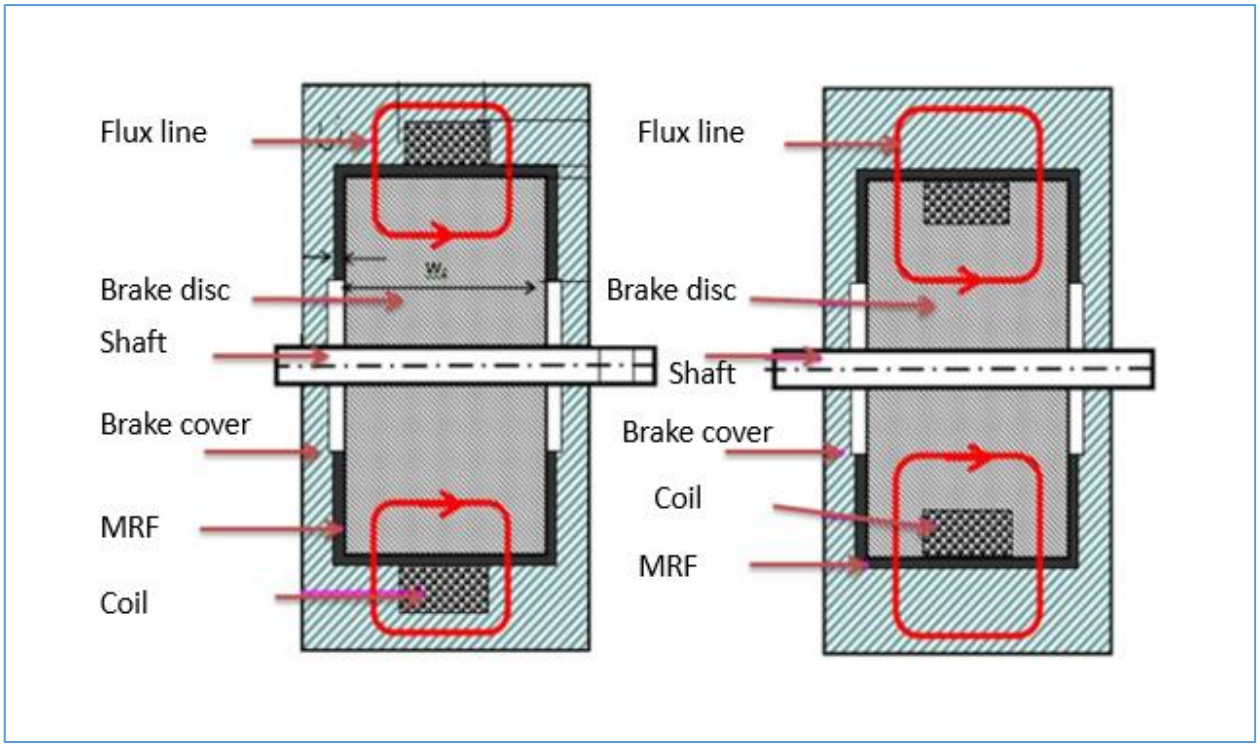

Figure 2- 10: Drum brake

Hybrid brake: is the type of break that combines disk type and drum type MRB. Therefore, it can overcome the disadvantages of the two types of brakes above. In fact, research shows that the hybrid brake is more optimal.

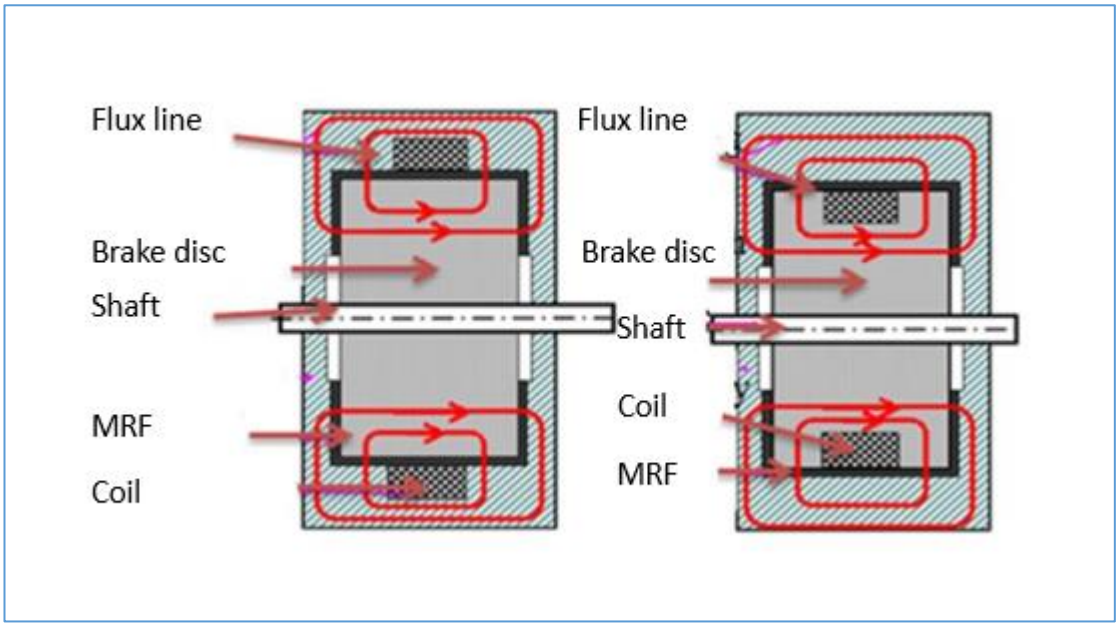

Figure 2- 11: Hybrid brake

In order to further optimize the performance of brakes, some other types of brakes based on hybrid brake were also studied such as hybrid brake with 2 coils and hybrid brake with a T-shaped rotor section

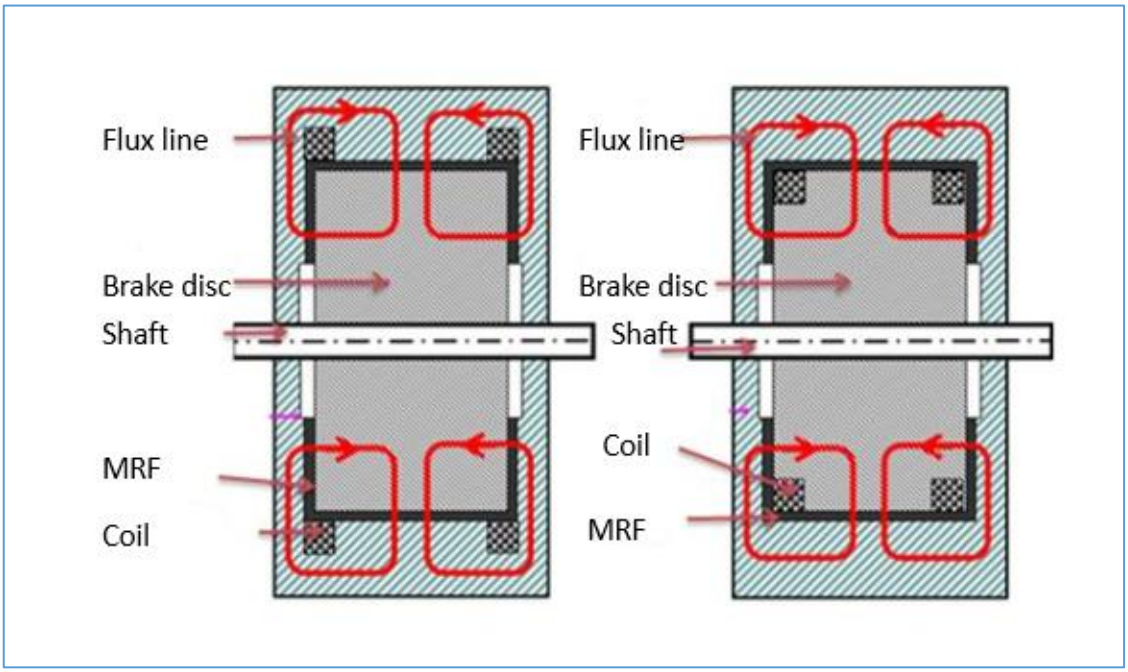

Figure 2- 12: Hybrid brake with 2 coils

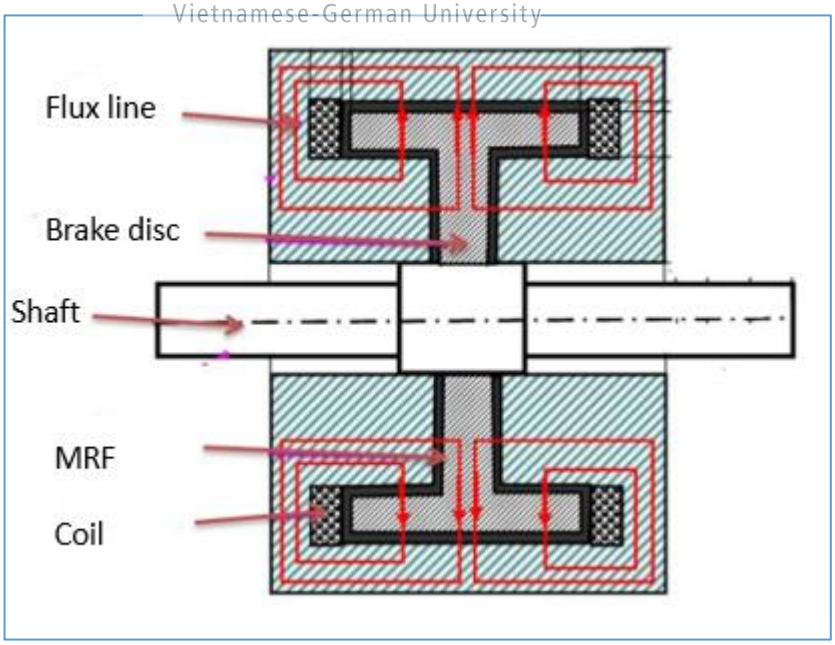

Figure 2- 13: Hybrid brake with T-shaped rotor section

2.6 Previous studies on MRF brakes

Currently, there are many studies in the world related to MRF brake such as

- Kerem Karakoc and associates: has proposed and designed MRF brakes to use for cars.
- Park and associates: research MRF brakes for use in automobiles
- Q H Nguyen, V T Lang, N D Nguyen and S B Choi, in 2013: MRB has been optimized for different shapes of brake covers.

Some traditional disc brakes, drum brakes, and combination brakes are often bulky in size and volume. On the other hand, studies of brakes with side coils also show that they are easy to make, simple, but the actual mass and dimensions have not changed significantly. However, this type of brake structure is very convenient for applying brakes with jig-jag magnetic flux lines to increase the brake moment and reduce its volume and size. Figure 2-14 depicts the MRF brake with jig-jag magnetic flux lines.

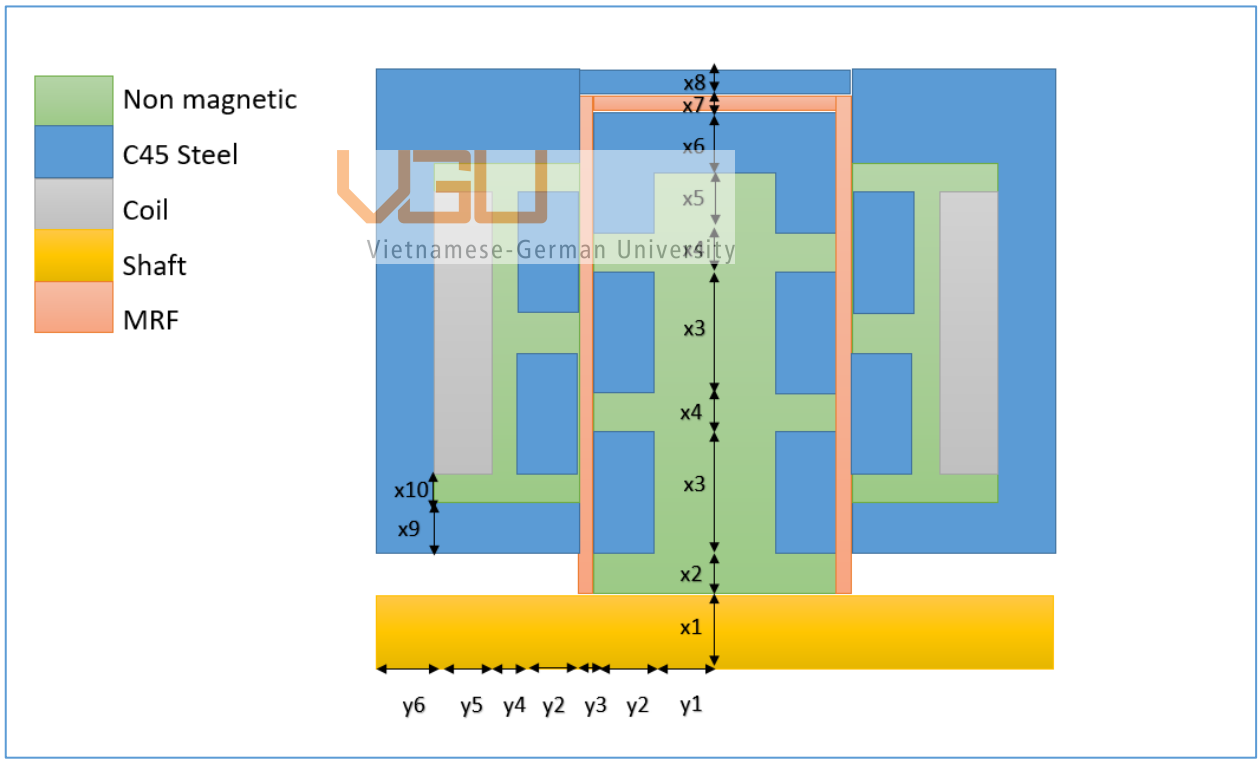

Figure 2- 14: Recommended MRB configuration

3. Magnetorheological fluid brake with jig-jag magnetic flux line

3.1 Selecting MRF

Currently, Lord Corporation is far ahead of other MRF manufacturers, with the following three types of MRF fluids:

- MRF-122-2ED: has small yield stress so it does not provide enough moment for MRF brake.
- MRF-132DG: has medium yield stress suitable for MRB
- MRF-140CG: has medium yield stress, high friction so it is not suitable for MRB

In this topic, we choose and use MRF-132DG as the most suitable. The parameters of MRF-132DG are shown in the following table:

Table 3- 1: MRF-132DG parameters

Property	Value/limits
Base fluid	Hydrocarbons
Operating temperature	-40 to 130 (°C)
Density	3090 (kg/m^3)
Color	Dark gray
Weight percent solid	81.64 (%)
Coefficient of thermal expansion (calculated values) 0-50 (°C) 50-100 (°C) 100-150 (°C)	Unit volume per °C 5.5e-4 6.6e-4 6.7e-4
Specific heat at 25 (°C)	800 (J/kg K)
Thermal conductivity at 25 (°C)	0.25-1.06 (W/m K)
Flash point	-150 (°C)
Viscosity (slope between 800 and 500 Hz at 40 (°C)	0.09 (±0.02) Pa s
k	0.269 (Pa m/A)
β	1

The magnetic characteristic of MRF-132DG is nonlinear and is defined by the B-H curve as follows:

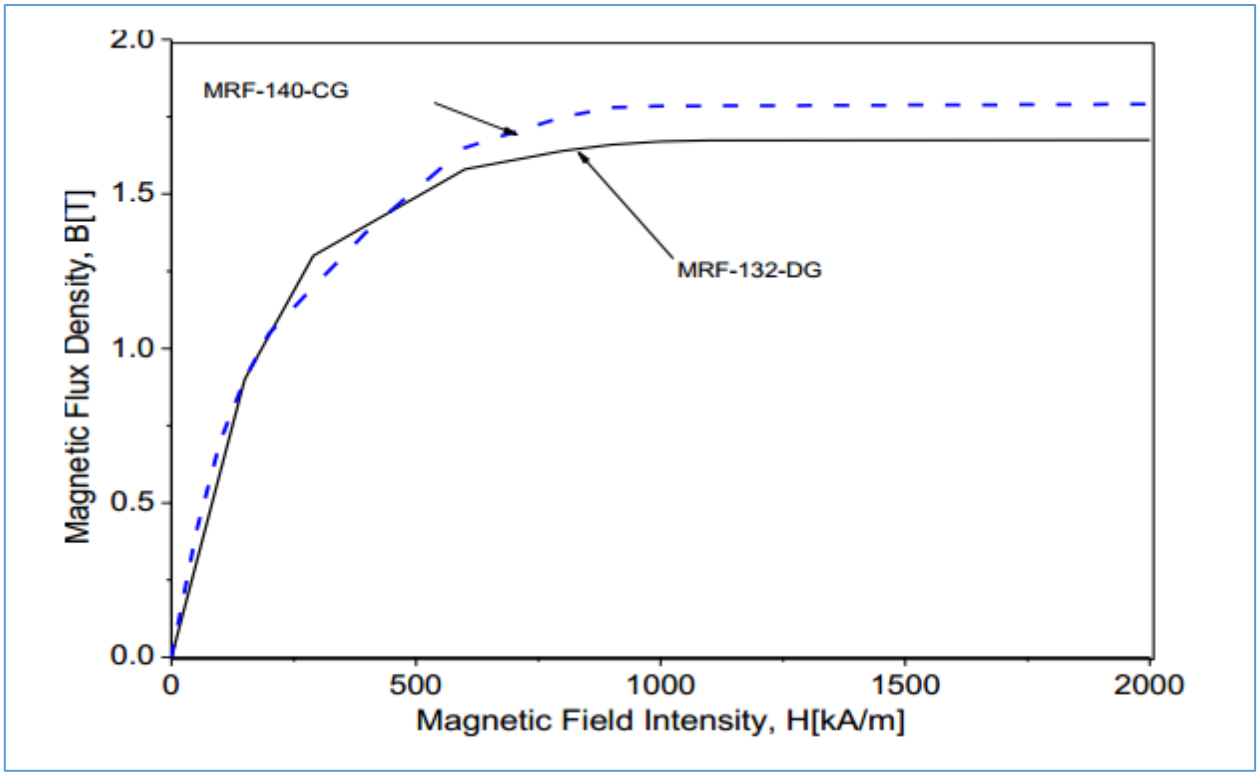

Figure 3- 1: B-H curve of MRF 132-DG

3.2 Selecting brake material

The selection of brake materials is an important part of MRB design and manufacturing. Materials used in MRB design and manufacture must meet the working conditions, requirements for design, manufacture and common use in the market. In this study, the material is carbon steel C45

C45 steel is widely used in engineering in general and machine building in particular because: with good technology, easy to process, good magnetic conductivity cheap and easy to find. C45 steel is a good quality steel, with a carbon percentage of about 0.42 - 0.50%. In addition, in steel components C45 (calculated by weight) also: C = 0.4 -0.5%; Si = 0.17 - 0.37%; Mn = 0.50 - 0.80%; Ni = 0.3%; S = 0.045%; P = 0.045%; Cr = 0.3%;

The magnetic properties of C45 steel are expressed by the following B-H curve:

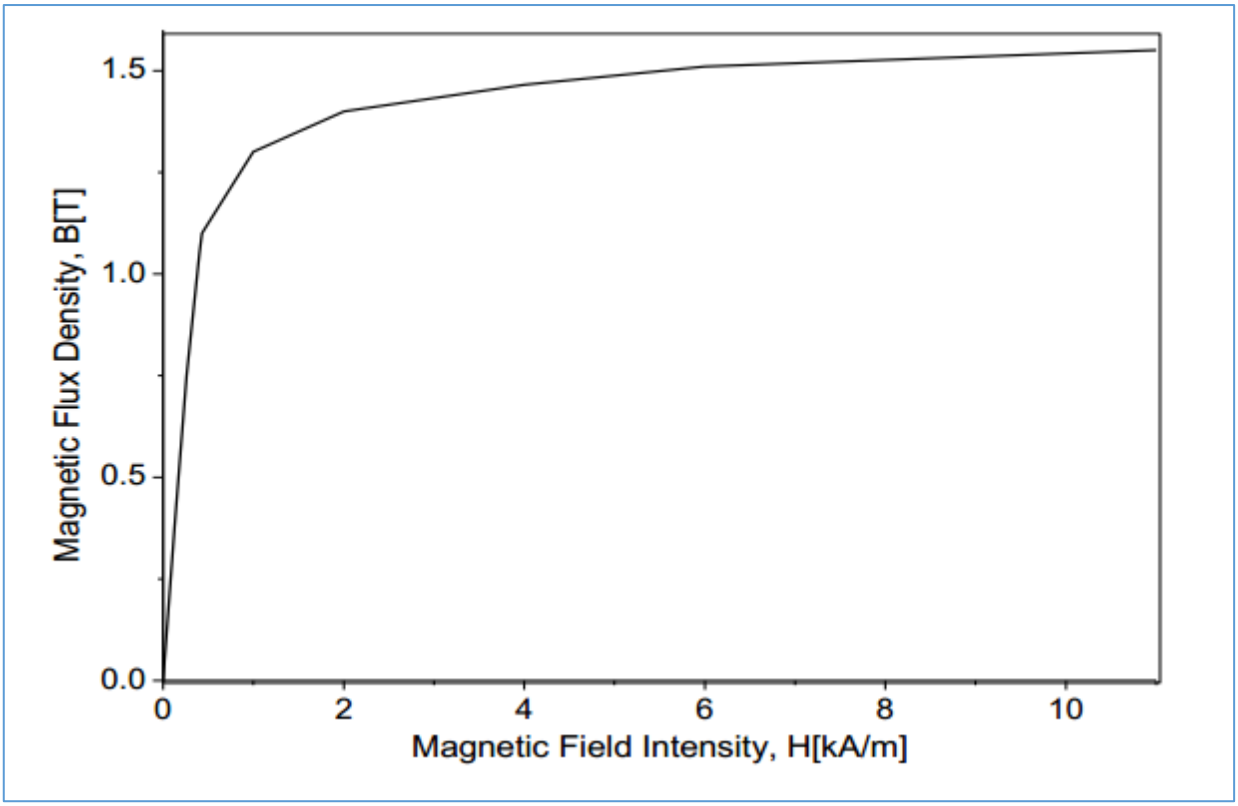

Figure 3- 2: B-H curve of C45 steel

3.3 Proposed MRF brake configuration

As presented in the previous section, to take advantage of disc brakes with side coils, simultaneously increasing the torque, reducing the braking volume; A new type of brake with jig-jag magnetic flux line is proposed as Figure 3-3. The proposed brake configuration includes the following parts:

- Brake covers: is a part that covers the whole brake, plays the role of holding the coil, creating a fluid slot with the disc, positioning the brake with the shaft.
- Coils: wrapped in accordance with the number of rounds calculated to provide a magnetic field for braking to operate in the presence of an electric current
- Fluid slot: created by the brake cover and brake disc to accommodate MRF.
- Brake disc: linked with shaft
- Shaft: has the duty to spin and drive the rotating disc.
- Bearings: separate movement from the shaft through the brake cover
- Seal: prevent magnetorheological fluid from leaking

Principle of operation: when the machine runs, it will make the shaft and disc rotate, the brake cover is fixed, at this time the current is not supplied to the coil, the fluid will move freely. In the event of a current, the coil creates a magnetic field that passes through the fluid slot, this time the MRF fluid coalesces to brake the disc, creating a brake moment that slows down the speed of the vehicle or stops the vehicle. Moment of braking is large or small depending on the magnitude of the amperage when feeding the coil.

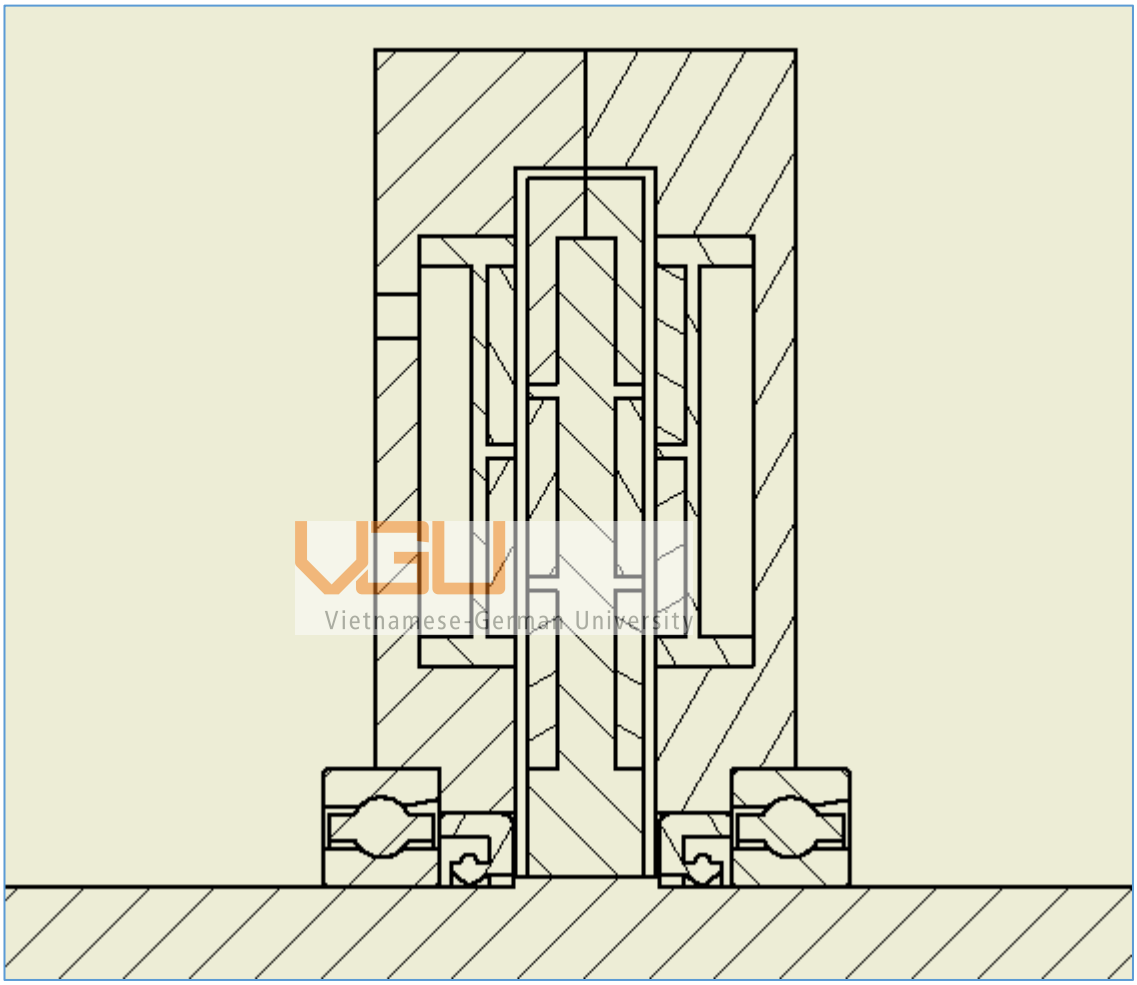

Figure 3- 3: Brake with jig-jag magnetic flux line

3.4 Calculating brake torque

In MRB design, the calculation of brake moment is extremely important, because it determines the braking efficiency. With the proposed brake, the braking torque is created in two different types of slits of the fluid flow as shown in Figure 3-4 include moment at a vertical cylinder A1, A2, A3, A4 and moment at a horizontal cylinder C

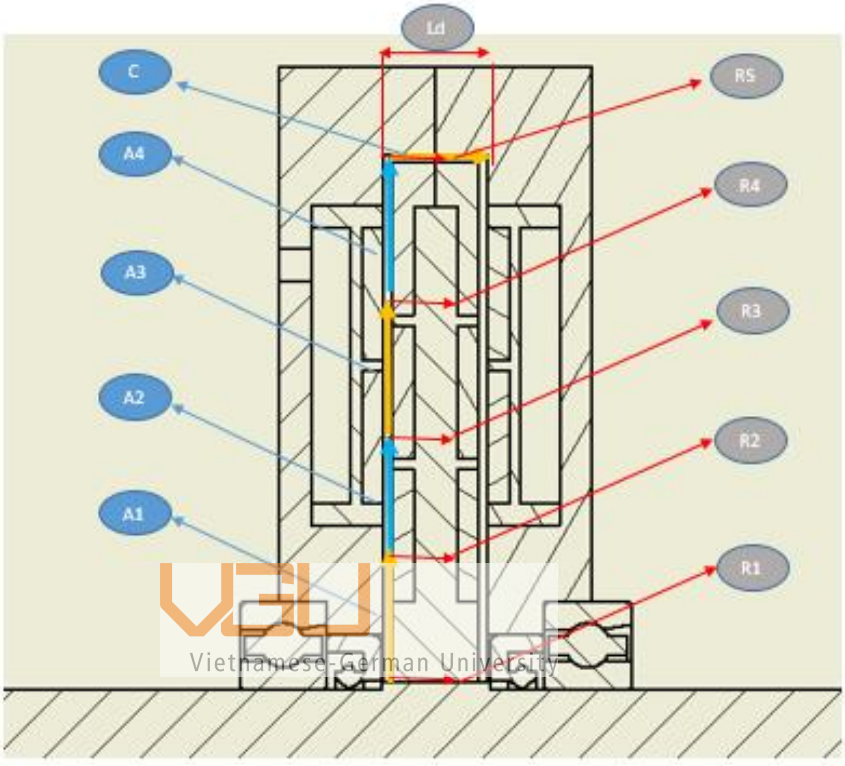

Figure 3- 4: Elements need to calculate MRB moment

Consider a small circular element of inclined groove as shown in Figure 3-5 with R1, R2 are the radius from ends of the slotted groove to the brake shaft; L_a is the length of a slotted projection on an axis; φ is the angle between the groove and the axis; l is the length of the groove

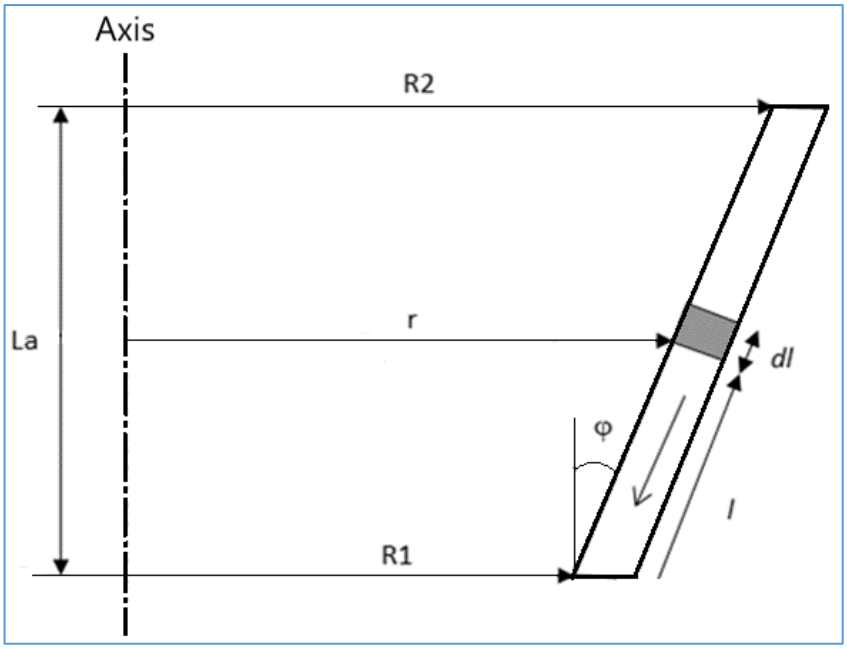

Figure 3- 5: An element needs to calculate the moment on the MRB brake disc

The instantaneous frictional force applied to this element is calculated by the formula:

$$dT = r\tau dA = 2\pi r^2 \tau dl = 2\pi(R_1 + l\sin\varphi)^2 \tau dl \quad (3\text{-}1)$$

To simplify the analysis of the moment of a disk MRB, the following assumptions are used:

- The fluid is uncompressed and the movement is stable in layers.
- The gravity and centrifugal force of moving fluid elements are not considered
- There is no radial velocity.
- The fluid is in full contact with the disc and does not slip
- Because the fluid slot is quite small, it is considered as the fluid filling completely and ignoring axial movement

With the assumptions made, the sliding speed of the fluid in the slot is calculated as follows:

$$\dot{\gamma} = \frac{r\Omega}{d} \quad (3\text{-}2)$$

In that formula, Ω is the angular velocity of the disc.

The Bingham model of MRB in axial direction is shown as follows:

$$\tau = \tau_y + \mu\dot{\gamma} = \tau_y + \mu\left(\frac{r\Omega}{d}\right) = \tau_y + \mu\left(\frac{(R_1 + lsin\varphi)\Omega}{d}\right) \quad (3\text{-}3)$$

Where τ: Shear stress

τ_y: Yield stress

μ: Viscosity

Substituting (2-6) into equation (2-4), we get:

$$T = 2\pi \int_0^{La/\cos\varphi} (R_1 + l\sin\varphi)^2 \tau dl = 2\pi \int_0^{l} (R_1 + l\sin\varphi)^2 \tau dl = 2\pi \int_0^{l} ({R_1}^2 + 2R_1 l\sin\varphi + l^2 sin^2\varphi)\tau dl$$

$$T = 2\pi \left({R_1}^2 l + R_1 l^2 \sin\varphi + \tfrac{1}{3} l^3 sin^2\varphi\right)\tau_y + 2\pi \int_0^{l} ({R_1}^2 + 2R_1 l\sin\varphi + l^2 sin^2\varphi)\mu \tfrac{\Omega(R_1 + l\sin\varphi)}{d} dl$$

$$T = 2\pi \left({R_1}^2 l + R_1 l^2 \sin\varphi + \frac{1}{3} l^3 sin^2\varphi\right)\tau_y + 2\pi\mu \frac{\Omega}{d} \int_0^{l} ({R_1}^2 + 2R_1 l\sin\varphi + l^2 sin^2\varphi)(R_1 + l\sin\varphi) dl$$

$$T = 2\pi \left({R_1}^2 l + R_1 l^2 \sin\varphi + \tfrac{1}{3} l^3 sin^2\varphi\right)\tau_y + 2\pi\mu \tfrac{\Omega}{d} \int_0^{l} \left({R_1}^3 + 3{R_1}^2 l\sin\varphi + 3R_1 {l}^2 sin^2\varphi + l^3 sin^3\varphi\right) dl$$

$$T = 2\pi \left({R_1}^2 l + R_1 l^2 \sin\varphi + \frac{1}{3} l^3 sin^2\varphi\right)\tau_y + 2\pi\mu \frac{\Omega}{d} \left({R_1}^3 l + \frac{3}{2}{R_1}^2 l^2 \sin\varphi + R_1 l^3 sin^2\varphi + \frac{1}{4} l^4 sin^3\varphi\right)$$

$$T = 2\pi \left({R_1}^2 l + R_1 l^2 \sin\varphi + \frac{1}{3} l^3 sin^2\varphi\right)\tau_y + \frac{1}{2}\pi\mu \frac{\Omega l}{d} (4{R_1}^3 + 6{R_1}^2 l\sin\varphi + 4R_1 l^2\, sin^2\varphi + l^3 sin^3\varphi)$$

For groove C (φ= 0°):

$$T = 2\pi({R_1}^2 l)\tau_y + \frac{1}{2}\pi\mu \frac{\Omega l}{d}\left(4{R_1}^3\right) = 2\pi({R_1}^2 l)\tau_y + 2\pi\mu \frac{\Omega l}{d}\left({R_1}^3\right)$$

$$T = 2\pi {R_1}^2 l(\tau_y + \mu R_1 \frac{\Omega}{d})$$

For groove A (φ= 90° and l = R_2 - R_1)

$$T = 2\pi({R_1}^2 l + R_1 l^2 + \frac{1}{3} l^3)\tau_y + \frac{1}{2}\pi\mu \frac{\Omega l}{d}(4{R_1}^3 + 6{R_1}^2 l + 4R_1 l^2 + l^3)$$

$$T = 2\pi(R_2 - R_1)\left({R_1}^2 + R_1(R_2 - R_1) + \frac{1}{3}(R_2 - R_1)^2\right)\tau_y$$

$$+\frac{1}{2}\pi\mu \frac{\Omega(R_2 - R_1)}{d}(4{R_1}^3 + 6{R_1}^2(R_2 - R_1) + 4R_1(R_2 - R_1)^2 + (R_2 - R_1)^3$$

$$T = 2\pi(R_2 - R_1)\left({R_1}^2 + R_1(R_2 - R_1) + \frac{1}{3}(R_2 - R_1)^2\right)\tau_y$$

$$+\frac{1}{2}\pi\mu \frac{\Omega(R_2 - R_1)}{d}(4{R_1}^3 + (R_2 - R_1)(3{R_1}^2 + 2(R_2 R_1 + {R_2}^2))$$

$$T = 2\pi(R_2 - R_1)\left({R_1}^2 + R_1(R_2 - R_1) + \frac{1}{3}(R_2 - R_1)^2\right)\tau_y$$

$$+\frac{1}{2}\pi\mu \frac{\Omega(R_2 - R_1)}{d}({R_1}^3 + {R_1}^2 R_2 + R_1 {R_2}^2 + {R_2}^3)$$

$$T = \frac{2}{3}\pi(R_2 - R_1)\left({R_2}^2 + R_1R_2 + {R_1}^2\right)\tau_y + \frac{1}{2}\pi\mu\frac{\Omega({R_2}^4 - {R_1}^4)}{d}$$

$$T = \frac{2\pi\tau_y}{3}\left({R_2}^3 - {R_1}^3\right) + \frac{\pi\mu\Omega({R_2}^4 - {R_1}^4)}{2d}$$

We have the moment at the grooves A as follows:

$$T_{A1} = \frac{\pi\mu}{2d}.\left[{R_2}^4 - {R_1}^4\right].\Omega + \frac{2\pi\tau_y}{3}.({R_2}^3 - {R_1}^3)$$

$$T_{A2} = \frac{\pi\mu}{2d}.\left[{R_3}^4 - {R_2}^4\right].\Omega + \frac{2\pi\tau_y}{3}.({R_3}^3 - {R_2}^3)$$

$$T_{A3} = \frac{\pi\mu}{2d}.\left[{R_4}^4 - {R_3}^4\right].\Omega + \frac{2\pi\tau_y}{3}.({R_4}^3 - {R_3}^3)$$

$$T_{A4} = \frac{\pi\mu}{2d}.\left[{R_5}^4 - {R_4}^4\right].\Omega + \frac{2\pi\tau_y}{3}.({R_5}^3 - {R_4}^3)$$

We have the moment at the grooves C as follows:

$$T_C = 2\pi.{R_5}^2.L_d.(\tau_y + \mu\frac{\Omega.L_d}{d})$$

So, the brake moment of MRB is:

$$T_B = 2(T_{A1} + T_{A2} + T_{A3} + T_{A4}) + T_C + 2.T_S$$

For T_S: moment generated by 2 seals, calculated by the formula:

$$T_S = (f_C.L_C + f_h.A_r).R_s$$

Where

L_C : is the frictional length of the seals surface

R_S : is the outer diameter of the seal.

f_C : is the friction per unit length of seal circumference caused by the compression ratio on the seal depending on the compression ratio of the seal and the hardness of the seal material.

f_h : is the frictional force of the seal due to the pressure of the fluid acting on the unit area of it. Since MRB operates on a shear-mode, the pressure applied by the MRF on the gasket is very small, so it can be ignored, f_h = 0.

A_r : is the inner diameter of the seal.

3.5 Calculate the magnetic brake field

3.5.1 Analytical methods

For an MRF-based system, two parallel problems are usually required: electromagnetic analysis and fluid system analysis. The magnetic circuit in the system can be solved according to Kirchoff's law through a formula:

$$\sum H_k . l_k = N_{turns} . I \tag{3-4}$$

Where: H_k is the strength of the magnetic field at the k[th] link of the circuit

l_k is useful length of that link

N_{turns} is the number of turns of the coil.

I is amperage

The magnetic flux of an electrical circuit is calculated using the formula:

$$\Phi = B_k . A_k \tag{3-5}$$

Where: Φ is the magnetic flux of the circuit

B_k is magnetic flux density at the k[th] link

A_k is cross sectional area at the k[th] link

On the other hand, B_k flux density is proportional to the magnetic field intensity H_k according to the formula:

$$B_k = \mu_0 . \mu_k . H_k \tag{3-6}$$

Where: μ_0 is the permeability of free space ($\mu_0 = 4\pi 10^{-7}$ *Tm/A*)

μ_k is the relative permeability of the material at the k[th] bond

When the magnetic field is large enough, it can magnetize materials and materials almost become magnets. Normally, the magnetic properties of materials can be expressed through B-H curves. When the magnetic field is low, considering the linear relationship, the magnetic flux density, and the magnetic field strength at the k[th] link can be approximated as follows.

$$B_k = \frac{\mu_0 . N_{turns} . I}{\frac{l_k}{\mu_k} + \sum_{i=1, i\neq k}^{n} \frac{l_i . A_k}{\mu_i . A_i}} \quad (3\text{-}7)$$

$$H_k = \frac{N_{turns} . I}{l_k + \sum_{i=1, i\neq k}^{n} \frac{\mu_k . A_k}{\mu_i . A_i} . l_i} \quad (3\text{-}8)$$

For MRF, the construction material is homogeneous, then: $\mu_1 = \mu_2 = \mu_3 = \ldots = \mu_n$ Thus, the magnetic flux density and the magnetic field strength passing through the active volume of MRF can be calculated as follows:

$$B_{mr} = \frac{\mu_0 . N_{turns} . I}{\frac{l_{mr}}{\mu_{mr}} + \frac{1}{\mu} \sum_i \frac{l_i . A_{mr}}{A_i}} \quad (3\text{-}9)$$

$$H_{mr} = \frac{N_{turns} . I}{l_{mr} + \frac{\mu_{mr} . A_{mr}}{\mu} \sum_i \frac{l_i}{A_i}} \quad (3\text{-}10)$$

Where: μ_{mr} is the relative permeability of MRF

μ is the relative permeability of materials

To apply the analytical method, we must assume the magnetic properties of the materials are linear (the B-H line is the straight line). Besides, to ensure accuracy, we divide the magnetic circuit of the brake into several small segments.

3.5.2 Finite element method

The advantage of analytical methods is a simple calculation. However, the results are not accurate. To ensure accuracy, the magnetic problem of MRF brakes can also be solved using the finite element method (FEM). In this study, I used ANSYS software to solve the braking magnetic field problem. In particular, the element used is plane 13 symmetric multi-field element plane.

3.6 Optimal calculation and brake mechanism design

3.6.1 Braking optimization design problem

In this section, the optimization of MRB is considered. The braking moment and the mass of the MRB are two important factors that their goals oppose. Specifically, the MRB should be as small as possible to minimize its size and cost in providing a brake moment. Therefore, the goal of MRB's optimal design is to find the lightest MRB structure that can produce the required brake moment.

In general, the MRB optimum design is MRB mass optimization and can be expressed as follows:

$$m_b = V_b . \rho_b \quad (3\text{-}11)$$

Where: m_b is the mass of MRB

V_b is the volume of MRB

ρ_b is the density of MRB

Thus, the optimal design of MRB is to find optimal sets of values of important dimensions of MRB such as disc thickness, disc radius, shell radius, brake length, coil thickness, coil width so that makes the braking torque reach the requirement and the braking volume is minimal. With the proposed research scope, in this topic, we will investigate the optimal moment at about 10 N.m

3.6.2 Method to solve the optimization problem

After determining the target function, the design parameters, we need to have the appropriate optimal method to achieve the desired optimal results.

There are many methods to find optimal results for the same problem: non-derivative, first derivative, second derivative. The non-derivative method does not require derivative but is not used in the MRF application because it is easy to implement but convergence is quite low with some specific functions such as Simplex, Neural Networks. The second derivative method with fast convergence ability and invariant mapping but this method requires quadratic derivatives and solutions of linear equations that are difficult to determine. The most popular optimal method for MRF applications is the first derivative, although the convergence rate is longer than the second derivative method it is still widely used as well as easy in programming calculations. A typical optimal algorithm of the first derivative method is the conjugate gradient

method. Flowchart figure 3-6 shows how the Ansys finite element software finds optimal results using the first derivative method.

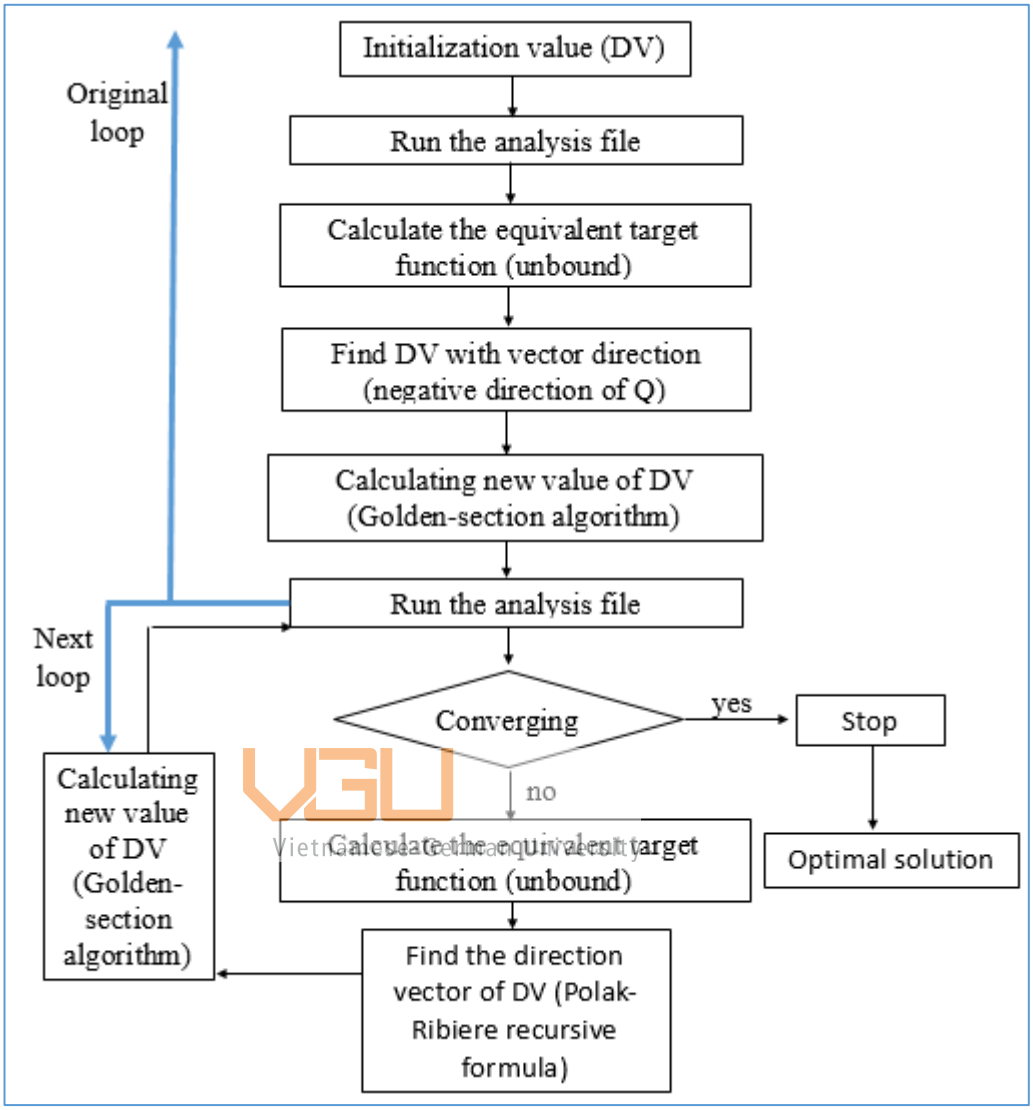

Figure 3- 6: Optimal design flowchart of MRF equipment using FEM

First, the value of the DV initialization variables will be determined. The computation time of the optimization process depends heavily on these values. Therefore, the initial value of the design variables will be calculated in advance or based on practical experience. Typically, to determine the operational characteristic of MRB, the magnetic flux density across the working volume of MRF will be calculated. The magnetic flux density B and electromagnetic stress H in the fluid gap are not constant, so when calculating we will use their average value. The average value of B and H across the fluid gap is calculated by taking the integral of the magnetic flux density along the predetermined path, then divide by the length of that path. To calculate the inductance time constant, the magnetic flux is first determined by the formula:

$$\Phi = 2\pi R_d \int_{L_p} B(s)ds \tag{3-12}$$

Where: $B(s)$ is the magnetic flux density at each node on the curve

S is the dummy variable for the integral.

The integration is performed along the L_p length of the curve. Besides, since the geometry of the MRB will change during the optimization process, the mesh size of the finite element model will be determined by the number of elements in a straight line instead of the size of that element. After the preparation of the analytical data, the process to obtain the optimum design parameters of the MRF brake using the first-order method of the ANSYS optimization tool is carried out as shown in Figure 3-6. Starting with the initial value of the design variables, by running the analysis file, we obtain the initial value of the brake operating characteristics such as control energy, inductance time constant, moment brake. After that, the ANSYS optimization tool will convert the constrained optimization problems into non-constrained via the penalty function. The unbound equivalence function has the following equation:

$$Q(x,q) = \frac{OBJ}{OBj_o} + \sum_{i=1}^{n} P_x(x_i) + q\sum_{i=1}^{m} P_g(g_i) \tag{3-13}$$

Where: OBj_o is reference target values

Q is the feedback surface parameter to accommodate constraints

P_x is outer penalty function, applies to variable x

P_g is an extended internal penalty function, applied to the g state variable

For the first loop (j = 0), finding the value of DV is assumed to be a negative direction gradient of the unbound target function. Therefore, the directional vector is calculated by the formula:

$$d^{(0)} = -\nabla Q(x^{(0)}, 1) \tag{3-14}$$

The values of DV in subsequent loops are found by the following formula:

$$x^{(j+1)} = x^j + s_j d^{(j)} \tag{3-15}$$

In particular, the s_j search parameter is calculated using a combination of the Golden-section algorithm and the local quadratic fitting technique. The analysis file is then executed with the new DV value and tested for convergence of the target function. If convergence occurs, the value of DV at the j^{th} loop is the optimal value; otherwise, the next loop will be executed. In the next loop, the process is similar to the first loop, except the quadratic vector is calculated using the Polak-Ribiere recursive formula:

$$d^{(j)} = -\nabla Q\left(x^{(j)}, q_k\right) + r_{j-1} d^{(j-1)} \tag{3-16}$$

$$r_{j-1} = \frac{\left[\nabla Q\left(x^{(j)}, q\right) - \nabla Q\left(x^{(j-1)}, q\right)\right]^T \nabla Q(x^{(j)}, q)}{|\nabla Q(x^{(j-1)}, q)|^2} \tag{3-17}$$

In ANSYS software, there is support for optimal design problems with the built-in optimization tool. Therefore, in most cases, the optimal problem of MRF devices can be solved directly by ANSYS software without having to go through any other programming software. However, in some cases, it is still necessary to use high-level optimization algorithms such as genetic algorithm, Neural Network or combination of ANSYS with other software to optimize such as Matlab, Fortran or C language.

3.6.3 Results of optimal braking problems

As the scope of the study has set out, this section not only explains the optimal results for the MR brake with jig-jag magnetic flux line but also finds and compares the optimal results of the previous MRB types such as single side-coil MRB, two coils on each side of the housing, three coils on each side of the housing, at 7 moments levels 5, 10, 20, 40, 60, 80, 100 Nm

Figure 3-7, Figure 3-8 and Figure 3-9 describe the structure and working principle of single side-coil MRB, two coils on each side of the housing and three coils on each side of the housing

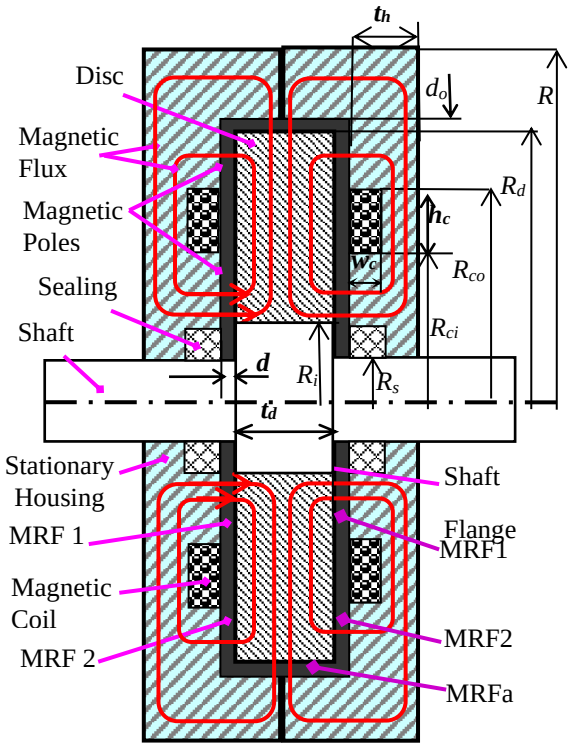

Figure 3- 7: Configurations of the single side-coil MRBs

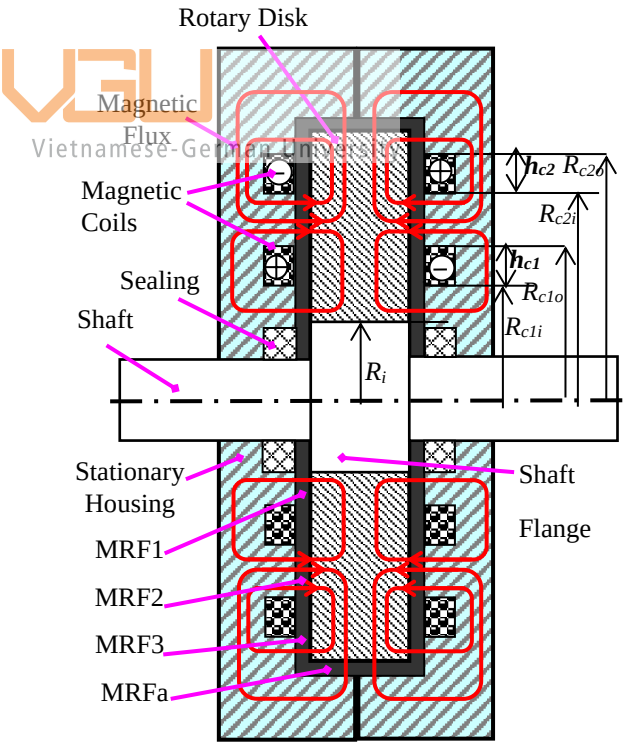

Figure 3- 8: Configurations of two coils on each side of the housing MRB

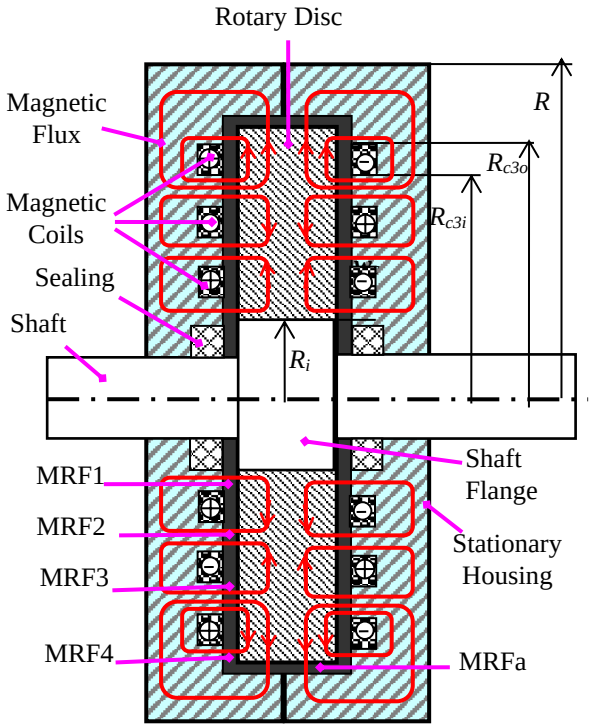

Figure 3- 9: Configurations of three coils on each side of the housing MRB

Data programming of optimal calculation MRB in Ansys is presented in Appendix 1. Some FEM models used in the magnetic field optimization problem are present as follows:

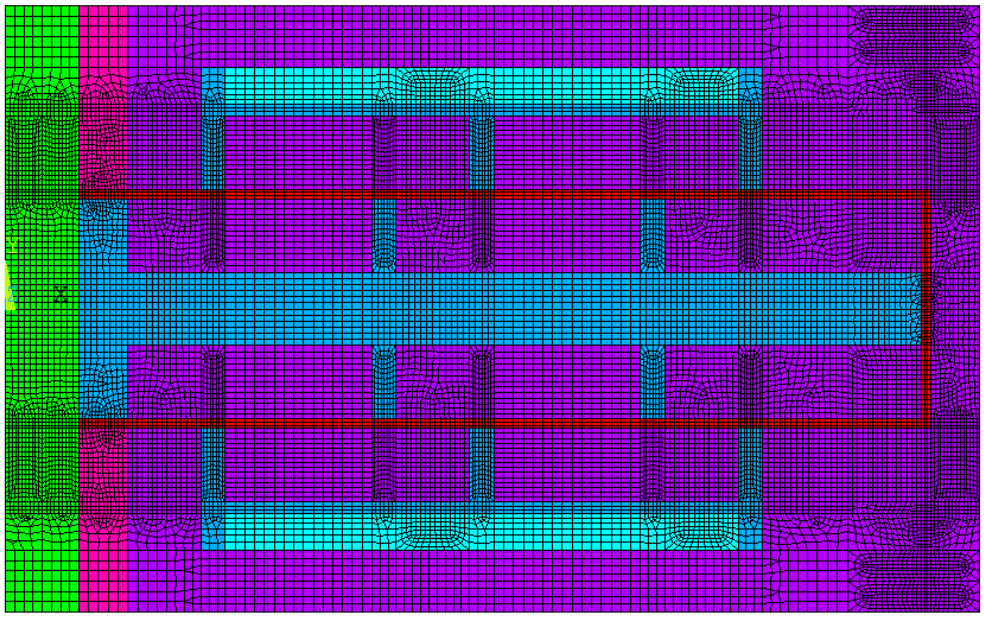

Figure 3- 10: Finite element models of MR brake with jig-jag magnetic flux line

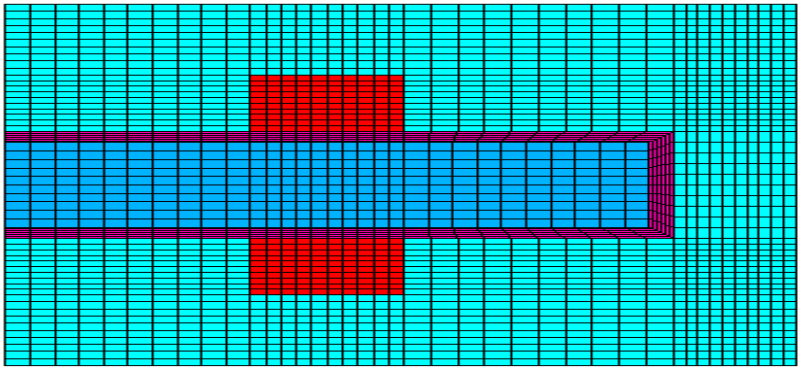

Figure 3- 13: Finite element models of the single side-coil MRBs

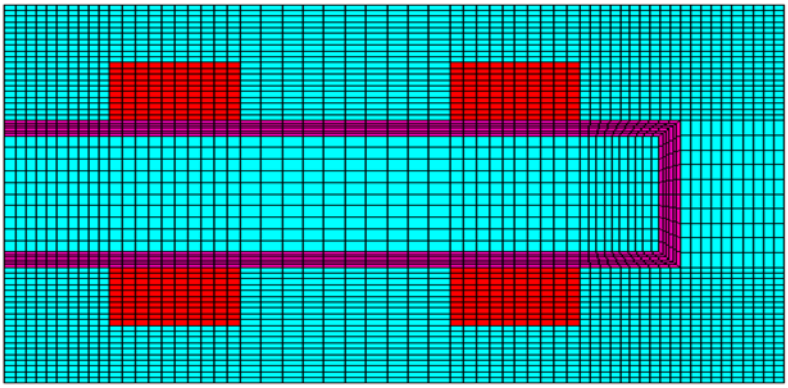

Figure 3- 12: Finite element models of two coils on each side of the housing MRB

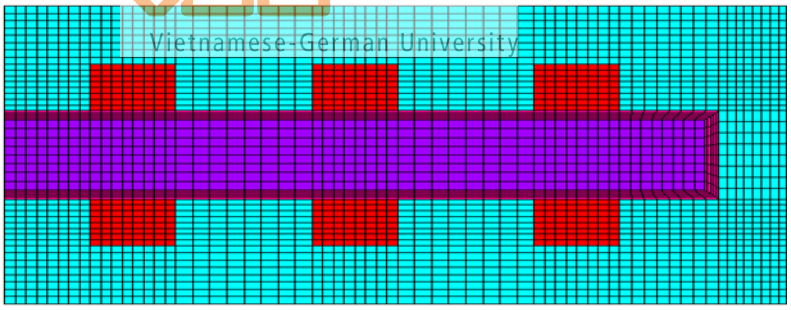

Figure 3- 11: Finite element models of three coils on each side of the housing MRB

After the optimum running of the MRB types with the material as mentioned previously at the torque level with 25 iterations, the relationship of mass, outside brake radius is shown as follows

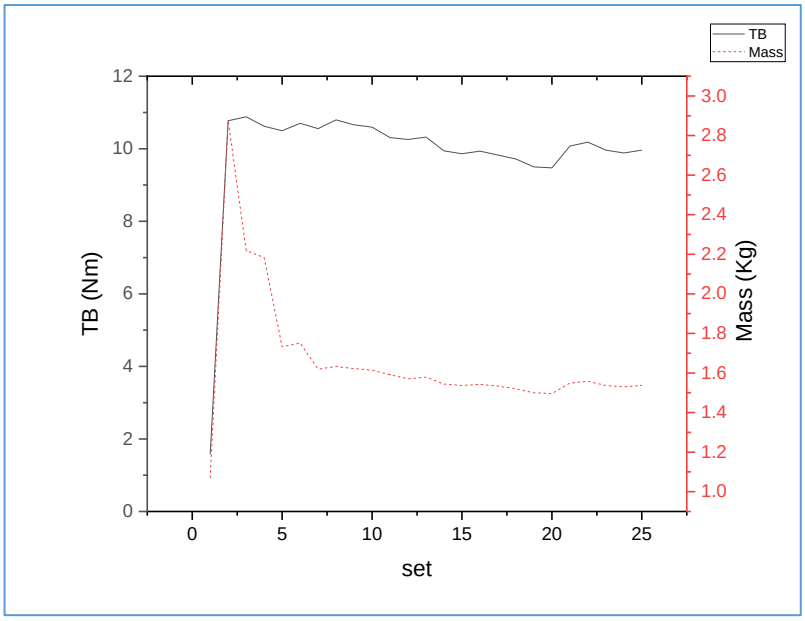

Figure 3- 14: Iteration of MR brake with jig-jag magnetic flux line

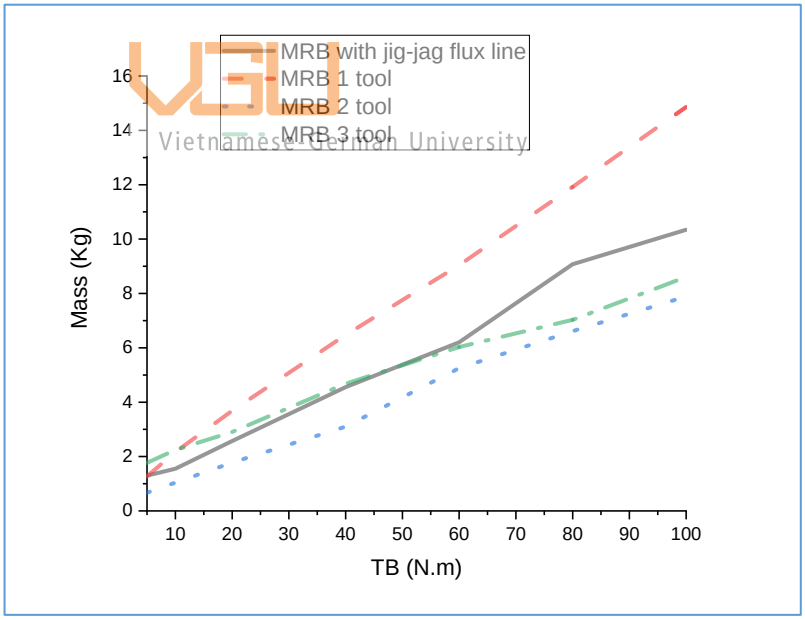

Figure 3- 15: Mass according to brake torque

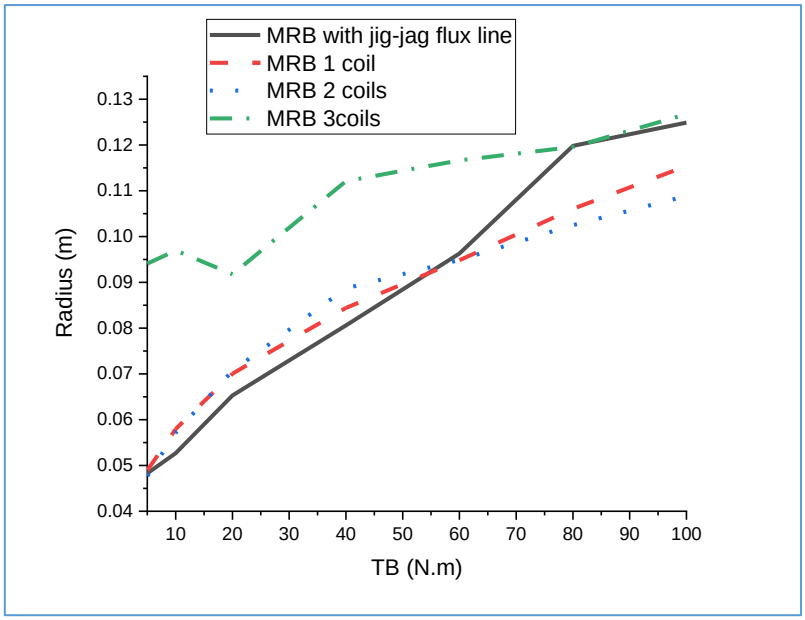

Figure 3- 16: Radius according to brake torque

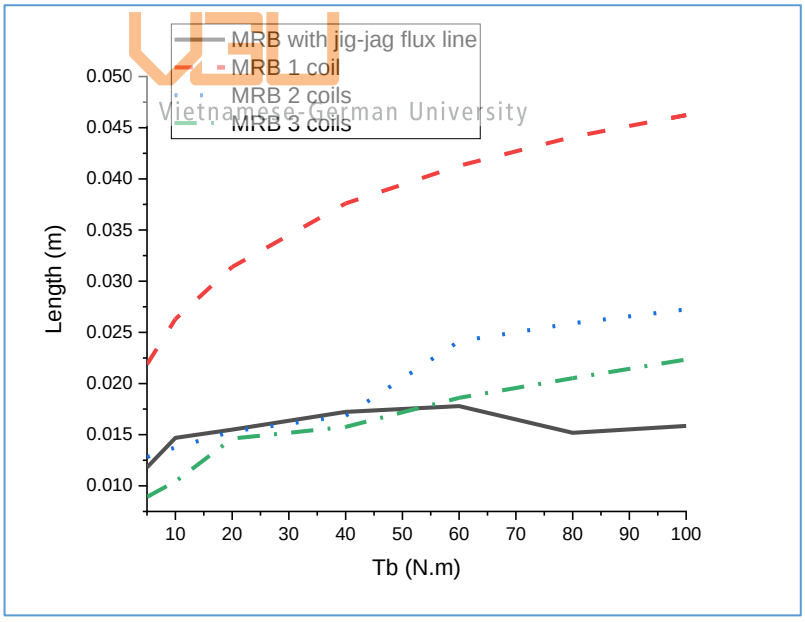

Figure 3- 17:Length according to brake torque

For a more general view of optimal braking, Figure 3-18 describes the magnetic field lines in the optimum brake and Figure 3-19 shows the magnetic distribution of the brakes as follows:

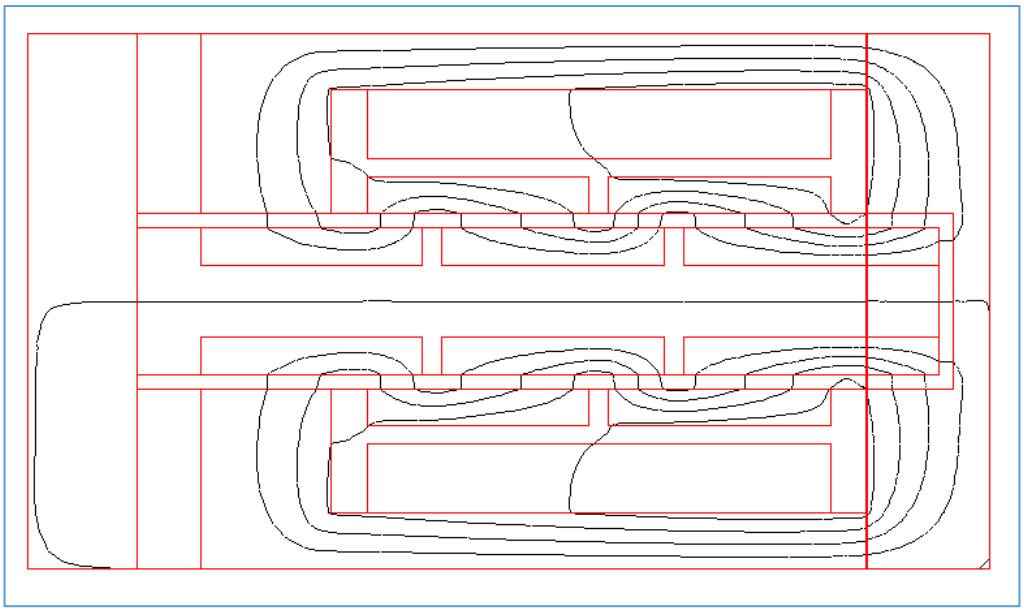

Figure 3- 18: Magnetic field distribution through fluid slits

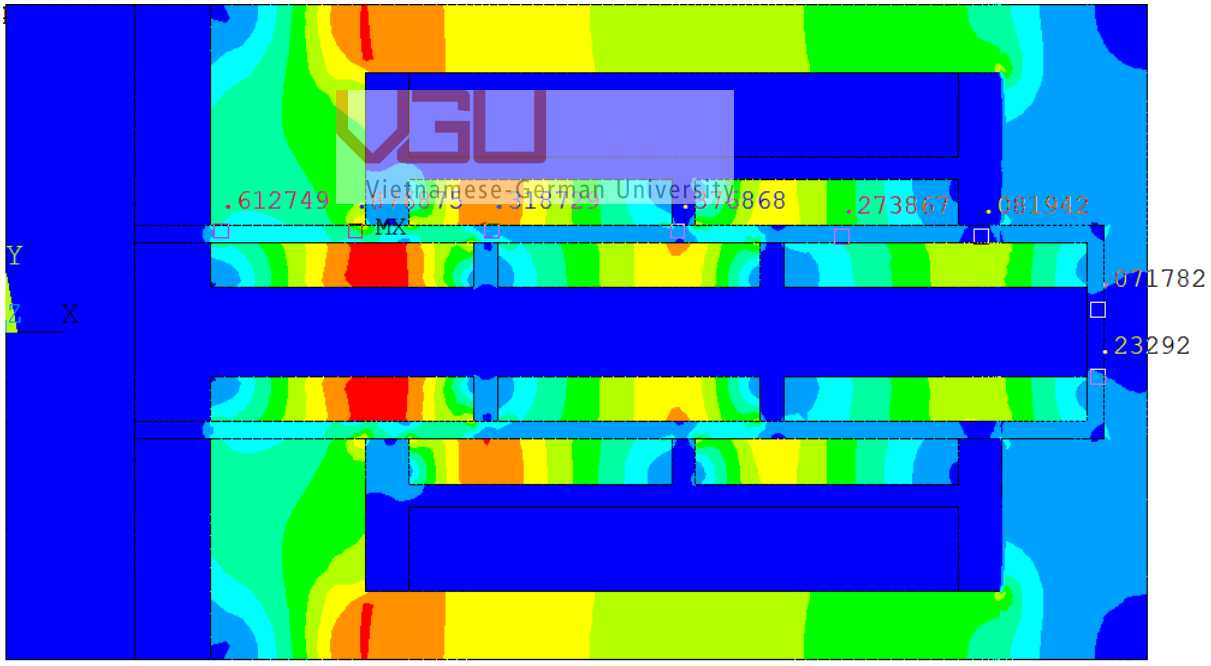

Figure 3- 19: Magnetic density distribution through the fluid slits

Optimal braking results are recorded and presented in detail in Table 3-2. This is the basis to evaluate the optimum of the proposed MRB.

Table 3- 2: Optimal result of MRB

MRB Type	Optimal design size (mm)	Optimal results
MR brake with jig-jag magnetic flux line	**Coils:** width w_c= 3.6; height h_c= 25; number of rounds nturns= 252 **Brake cover**: radius r =132.4, width w= 14.4 **Disc:** radius r = 100, width w = 8 MRF slits: 0.8	**Brake torque:** 10 N.m **Mass:** 1.54 Kg

3.6.4 Brake mechanism design

Based on the optimum results and for the convenience of the mounting, the brake structure is designed. Figure 3-20 shows the overall structure and installation drawings of the brake designed in this study

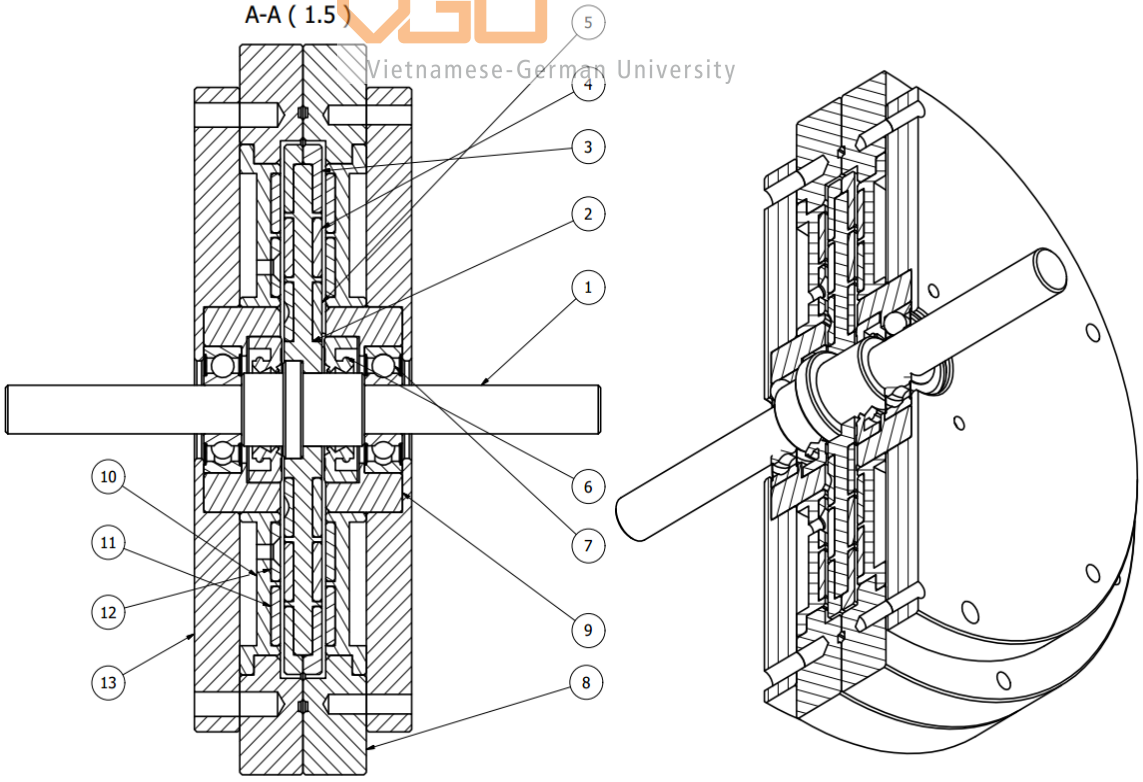

Figure 3- 20: Overall structure and drawings of the brake

Table 3-3 shows the part list of MRB:

Table 3- 3: Parts list

Number	Part name	Unit
1	Shaft	1
2	Brake disc	1
3	Magnetic plate 2	2
4	Magnetic plate 3	2
5	Magnetic plate 1	2
6	Seal	2
7	Bearing	2
8	Brake cover 1	2
9	Brake cover 2	2
10	Brake pad	2
11	Magnetic plate 4	2
12	Magnetic plate 5	2
13	Brake cover lid	2

Some detailed drawings of MRB's parts are as follows:

Brake disc:

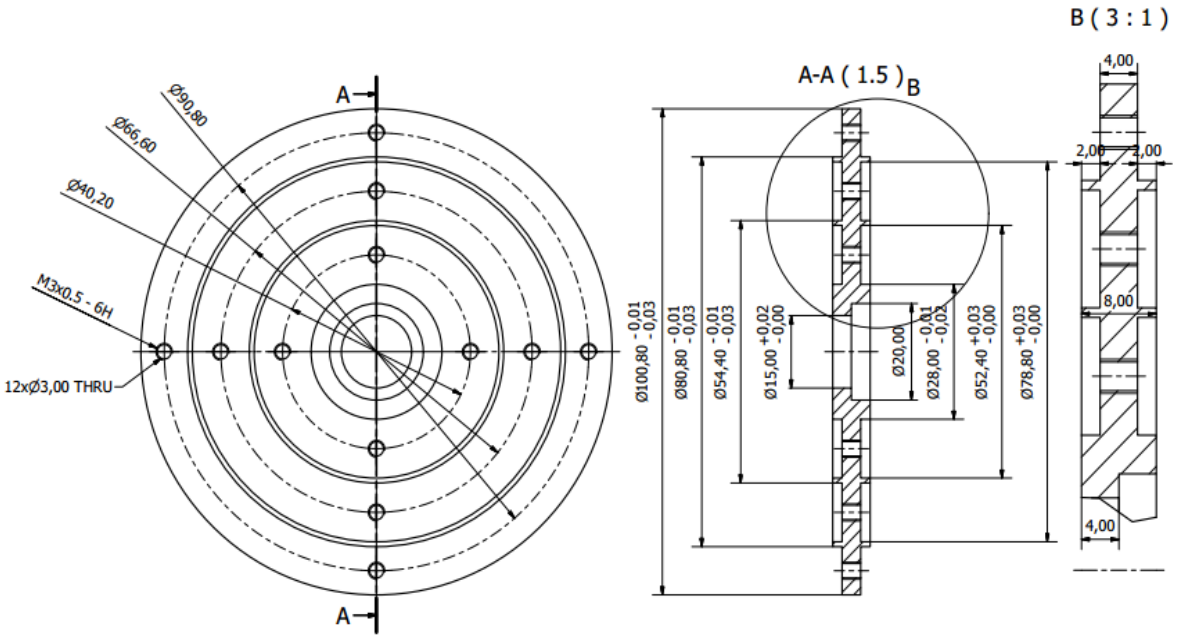

Figure 3- 21: Drawing of brake disk

Brake cover 1:

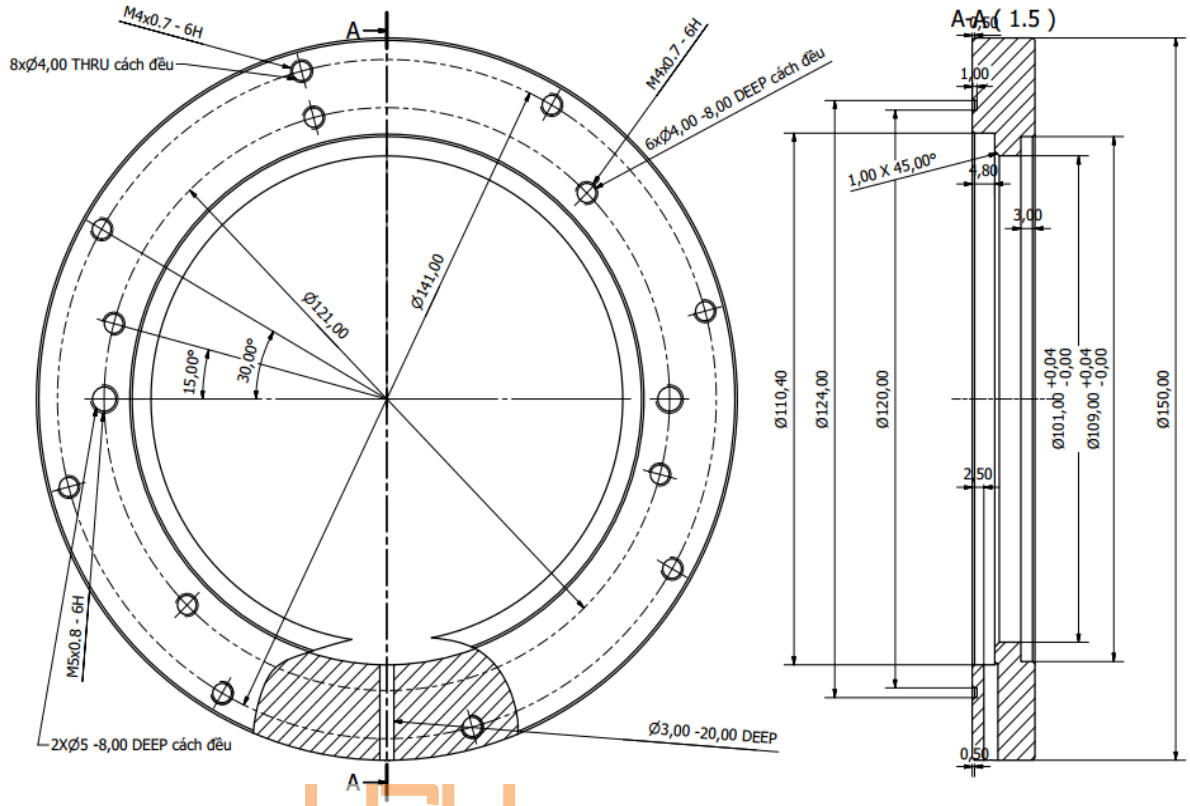

Figure 3- 22: Drawing of brake cover 1

Brake cover 2:

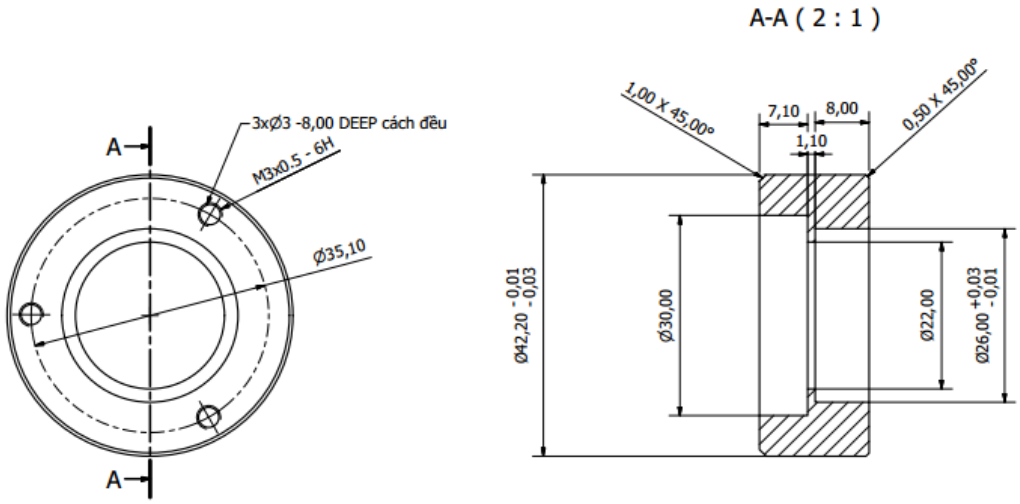

Figure 3- 23: Drawing of brake cover 2

Brake pad:

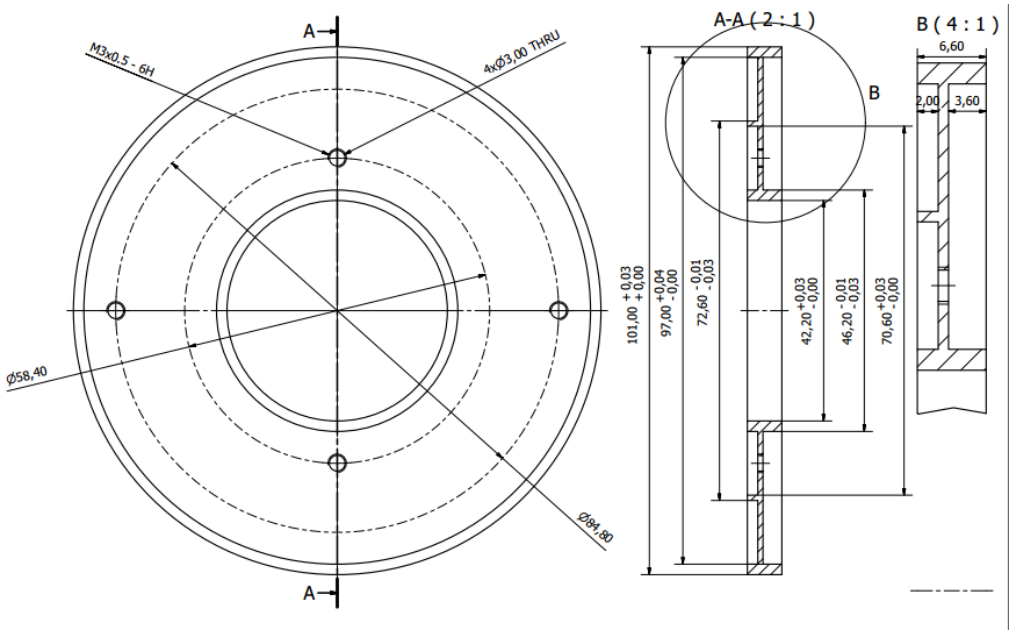

Figure 3- 24: Drawing of brake pad

Brake cover lid:

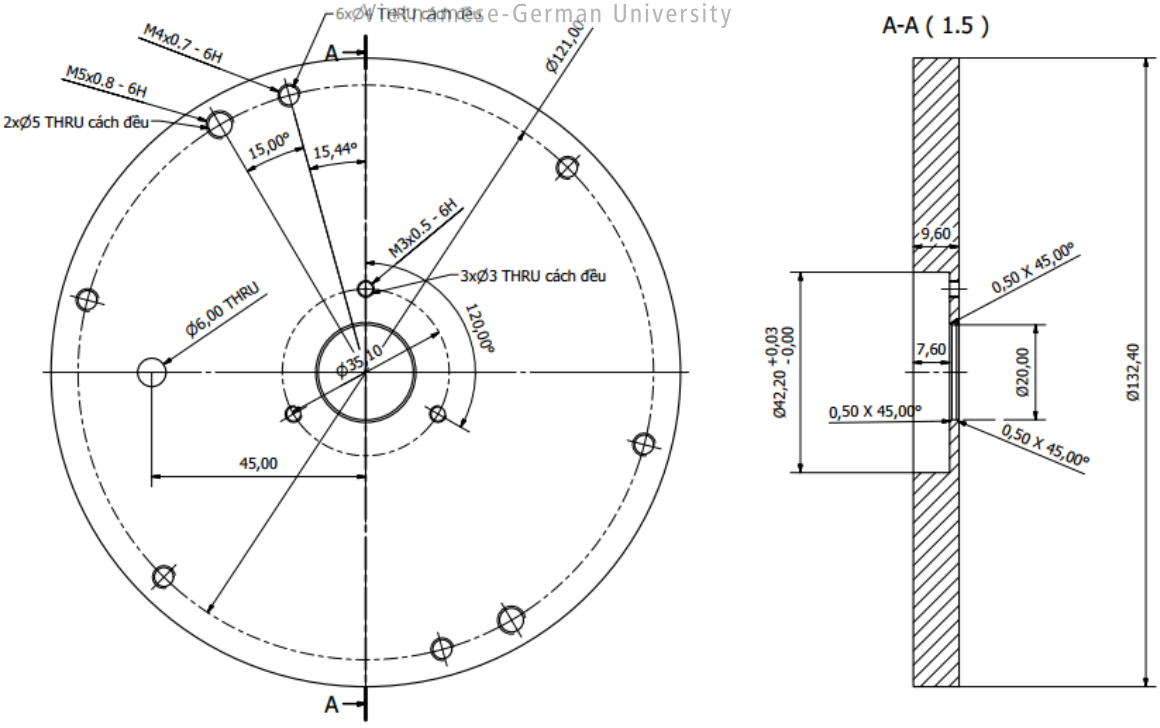

Figure 3- 25: Drawing of brake cover lid

Shaft:

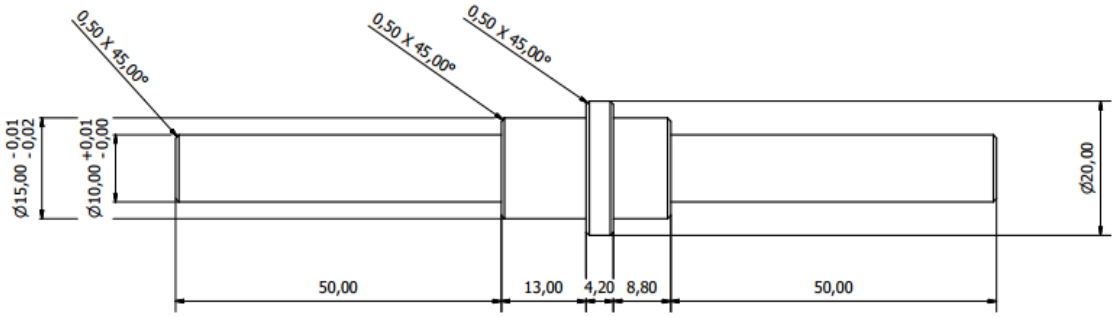

Figure 3- 26: Drawing of shaft

Magnetic plate 1:

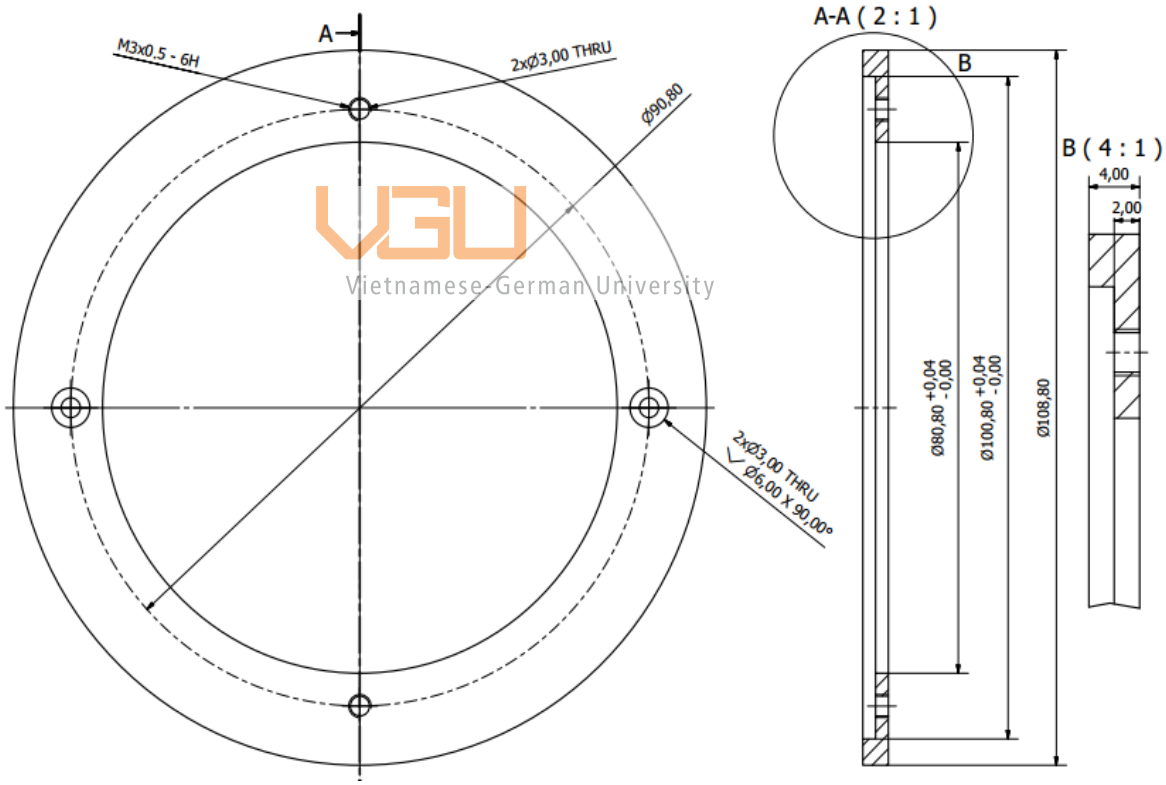

Figure 3- 27: Drawing of magnetic plate 1

4. Manufacturing MRF brakes

Fabrication of the brakes is done according to the design drawings. The process of making brakes is made on small orders, so the process takes many stages and processing time. However, when processing should be noted the following:

- Disc brake: must ensure high accuracy, correct shape, size, not deformed after machining.
- Brake shaft: plays a role in binding the dimensions of the brakes, so it needs high precision machining and removable capabilities.
- Brake pads: the two brake pads must ensure the accuracy as the brake disc, the processing should be carried out slowly to avoid deforming the brake pads because of the relatively small thickness, to ensure the brake profile as well as the gap of MRF.
- Coils: Coils must ensure the number of turns and fill in the wire frame
- Brake cover: The outer cover of the brake cover does not require high precision, so it can be machined on normal lathe machine. However, the inside requires precision in assembling, so it requires machining on CNC machines
- The brake assembly process is done manually. The brake pads are closed with ball bearings and seals. The disc is rigidly mounted on the shaft by welding. The coils are put into the groove and the glue is poured. The parts are assembled together, the contiguous area between the two brake covers is covered with a layer of waterproof glue to prevent fluid from flowing out, then use screws to attach the brake covers.
- When everything is satisfactory, I proceed to pump the fluid into the brake and then tighten the screw to avoid leakage

Some pictures of the parts after manufacturing:

Figure 4- 1: Brake cover lid front and back

Figure 4- 2: Brake pad front and back

Figure 4- 3: Brake cover 1 and 2

Figure 4- 4: Brake disc

Figure 4- 5: Magnetic plates

Figure 4- 6: Shaft

5. Conclusions and recommendations

The fundamental goal of this thesis, which is to produce a new type of MRB with jig jag flux line, was finally conducted in three months. The first month was for researching and reviewing the theory and previous studies to understand and design a product that fulfills the requirement of the MRB. Afterward, the calculation with the help of the ANSYS system and CAD tasks proceed contemporaneously because they affected mutually. After the above steps have been completed, I obtain the drawing and the brake specifications and start the manufacturing process. After getting the products through the manufacturing process, I buy the missing parts and assemble the brakes. Finally, the last two weeks were spent on reviewing and editing the thesis.

5.1 Conclusions

In this study, I have proposed, calculated, designed, compared to previous MRBs, manufactured MRBs with jig-jag flux line and the test showed that it has more advantages than previous types of brakes. In detail, for the same amount of torque generated, brake with jig-jag flux line has a significantly reduced mass compared to brake with 1 coil. For MRB with 2 coils and 3 coils, despite having a larger volume in some torque areas, MRB with jig-jag flux line has a smaller energy consumption

With this new profile, the research has launched a new generation of brakes to overcome the disadvantages of the previous types of brakes with smaller volumes with different torque levels while ensuring the fabrication.

5.2 Recommendations

Due to the limited time of research, the operation of brakes in practice has not yet been tested. Moreover, to make sure the brakes work properly in practice, the following factors need to be strictly tested: durability, reliability, life expectancy. The braking process takes time and money due to small orders. In the following studies, it is necessary to find ways to reduce processing costs, reduce machining time and easier assembly and removal of parts. The study of MRB with jig-jag flux line needs to be continued and developed to evaluate factors as well as economic efficiency to be able to put the product into practical use.

References

1. A. Spaggiari, Frattura ed Integrità Strutturale. (2013). Properties and applications of Magnetorheological fluids. *The Italian research on smart materials and MEMS*.

2. Brian E S. (2005). Research for dynamic seal Friction modeling in linear motion hydraulic Piston applications. *Master of Science thesis, University of Texas at Arlington, USA*.

3. Carlson, Daniel E Barber and J David. (2009). Performance Characteristics of Prototype MR Engine Mounts Containing LORD Glycol MR Fluids. *Journal of Physics*.

4. D. J. Klingenberg. (2001). Magnetorheology: Applications and Challenges. *AIChE Journal*.

5. Huang J, Zhang J Q, Yang Y and Wei Y. (2002). Analysis and design of a cylindrical magnetorheological fluid brake. *Journal of Materials Processing Technology*.

6. J., Rabinow. (1951). Magnetic fluid torque and force transmitting device. *US patent*.

7. Liu B, Li W H, Kosasih P B and Zhang X Z. (2006). Development of an MR-brake-based haptic device. *Smart Mater. Struct.*

8. Lord Corporation . (2018). *data sheet*. Retrieved from http://www.lordmrstore.com/lord-mr-products/mrf-132dg-magneto-rheological-fluid-250ml.

9. Monika Kciuk, Roman Turczyn. (2006). Properties and application of magnetorheological fluids. *Research gate*.

10. Nguyen Q H and Choi S B. (2012). Optimal design of a novel hybrid MR brake for motorcycles considering axial and radial magnetic flux. *Smart Materials and Structures*.

11. Nguyen Q H, Nguyen N D and Choi S B. (2014). Optimal design of a novel configuration of MR brake with coils placed on the side housings. *Proc. SPIE 9059, Industrial and Commercial Applications of Smart Structures Technologies*.

12. Nguyen Q. Hung and Choi S. Bok. (2012). Optimal Design of a T-Shaped Drum-Type Brake for Motorcycle Utilizing Magnetorheological Fluid. *Mechanics Based Design of Structures and Machines*.

13. Nguyen Quoc Hung, Nguyen Ngoc Diep, Nguyen Si Dung. (2015). Development of magnetorheological brake with two coils placed on each side of the brake housing. *Vietnam Journal of Mechanics*.

14. Q H Nguyen and S B Choi. (2010). Optimal design of an automotive magnetorheological brake considering geometric dimensions and zero-field friction heat. *Smart Mater. Struct*.

15. Q H Nguyen, V T Lang, N D Nguyen and S B Choi. (2014). Geometric optimal design of a magneto-rheological brake considering different shapes for the brake envelope. *Smart Mater. Struct*.

16. Quoc Hung Nguyen and Seung Bok Choi. (2008). Optimal design of a vehicle magnetorheological damper considering the damping force and dynamic range. *Smart Mater. Struct*.

17. Quoc Hung Nguyen, Seung Bok Choi and Norman M Wereley. (2006). Optimal design of magnetorheological valves via a finite element method considering control energy and a time constant. *Smart Mater. Struct*.

18. Quoc-Hung Nguyen and Seung-Bok Choi. (2012). Optimal Design Methodology of Magnetorheological Fluid Based Mechanisms. *Smart Mater. Struct*.

19. Smith A L, Ulicny J C and Kennedy L C. . (2007). Magnetorheological fluid fan drive for trucks. *Journal of Intelligent Material Systems and Structures*.

20. Zubieta M, Eceolaza S, Elejabarrieta M J and Bou-Ali M M. (2009). Magnetorheological fluids: characterization and modeling of magnetization. *Smart Materials and Structures* .

Appendix – Bill of materials

The list below just counts components which are not available in the laboratory of VGU department.

Material	Cost/unit (vnd)	Number
Manufacturing parts	8.500.000	1
Seals	20.000	2
Bearing	50.000	2
Coil	200.000	1
Glue	60.000	1
Total cost	8.900.000	

Statutory Declaration

I declare that the subject of this work is not identical to the subject of a work that I have already submitted for another exam.

I further declare that I have not already submitted the thesis to another university for an academic degree.

I assure you that I wrote the work independently and did not use any other sources than those indicated. This also applies analogously to delivered drawings, sketches and pictorial representations and the like.

_____ _____

Place, Date Signature